PNNL-11691
UC-2030

Self-Assembled Mercaptan on Mesoporous Silica (SAMMS) Technology for Mercury Removal and Stabilization

X. Feng
J. Liu
G. E. Fryxell
M. Gong
Li-Q. Wang
X. Chen
D. E. Kurath
C. S. Ghormley
K. T. Klasson
K. M. Kemner

September 1997

Prepared for the
U.S. Department of Energy
under Contract DE-AC06-76RLO 1830

DISTRIBUTION OF THIS DOCUMENT IS UNLIMITED

Pacific Northwest National Laboratory
Richland, Washington 99352

MASTER

DISCLAIMER

This report was prepared as an account of work sponsored by an agency of the United States Government. Neither the United States Government nor any agency thereof, nor Battelle Memorial Institute, nor any of their employees, makes **any warranty, express or implied, or assumes any legal liability or responsibility for the accuracy, completeness, or usefulness of any information, apparatus, product, or process disclosed, or represents that its use would not infringe privately owned rights**. Reference herein to any specific commercial product, process, or service by trade name, trademark, manufacturer, or otherwise does not necessarily constitute or imply its endorsement, recommendation, or favoring by the United States Government or any agency thereof, or Battelle Memorial Institute. The views and opinions of authors expressed herein do not necessarily state or reflect those of the United States Government or any agency thereof.

PACIFIC NORTHWEST NATIONAL LABORATORY
operated by
BATTELLE
for the
UNITED STATES DEPARTMENT OF ENERGY
under Contract DE-AC06-76RLO 1830

Printed in the United States of America

Available to DOE and DOE contractors from the Office of Scientific and Technical Information, P.O. Box 62, Oak Ridge, TN 37831; prices available from (615) 576-8401.

Available to the public from the National Technical Information Service, U.S. Department of Commerce, 5285 Port Royal Rd., Springfield, VA 22161

This document was printed on recycled paper.
(9/97)

DISCLAIMER

Portions of this document may be
illegible in electronic image products.
Images are produced from the best
available original document.

Self-Assembled Mercaptan on Mesoporous Silica (SAMMS) Technology for Mercury Removal and Stabilization

Principal Investigator and Project Manager:

Xiangdong Feng

Pacific Northwest National Laboratory
PO Box 999, P8-37
Richland, WA 99352
509-373-7284 (o), 509-376-1638 (f)
E-Mail: x_feng@pnl.gov

Co-Principal Investigators:

Jun Liu
Glen E. Fryxell

Investigators:

Meiling Gong
Li-Qiong Wang
Xiaobing Chen
Dean E. Kurath
Chris S. Ghormley

Collaborators:

K. Thomas Klasson
Oak Ridge National Laboratory

Ken M. Kemner
Argonne National Laboratory

This page(s) is (are) intentionally left blank.

Summary

Self-Assembled Mercaptan on Mesoporous Silica (SAMMS), a proprietary new technology (X Feng, J Liu, and GE Fryxell, *Self-assembled Mercaptans on Mesoporous Silica (SAMMS) for Mercury Separation and Stabilization,* U.S. Patent Application filed on February 7, 1997, PNNL #E-1479) for mercury removal from aqueous wastewater and mercury removal from organic wastes, such as vacuum pump oils, is being developed at Pacific Northwest National Laboratory (PNNL). SAMMS represents a new class of materials, (X Feng, GE Fryxell, LQ Wang, AY Kim, J Liu, and KM Kemner, 1997, "Functionalized Monolayers on Ordered Mesoporous Supports," *Science*, ***276***, 923-926) that integrates two frontiers of science: mesoporous ceramic materials (CT Kresge, ME Leonowicz, WJ Roth, JC Vartuli, and JS Beck. 1992. *Nature* **359:**710) and self-assembled organic monolayers (BC Bunker,, PC Rieke, BJ Tarasevich, AA Campbell, GE Fryxell, GL Graff, L Song, J Liu, and JW Virden. 1993. "Ceramic Thin Film Formation on Functionalist Interfaces Through Biomimetic Processing," *Science*, **261**, 1286). Mesoporous ceramics are materials in which the pore size, ceramic substrate, and geometry can be manipulated. Its narrow pore size distribution can be specifically tailored from 15 Å to 200 Å, and it provides a high surface area (>900 m^2/g) needed for high metal loading in chemical separation. Self-assembled monolayers of organic molecules bond to the ceramic substrate with prescribed densities and contain a free functional group that provides excellent molecular selectivity. The unique characteristics of SAMMS in mercury separation were studied at PNNL using simulated aqueous tank wastes and actual tritiated pump oil wastes from Savannah River Site (SRS); the preliminary results show that

- the apparent mercury absorption capacity was up to 0.64 g/g of SAMMS due to the high surface area of SAMMS (~ 1000 m^2/g)
- the Hg-binding kinetics were fast (this was shown by reducing a 0.5-ppm mercury solution down to 0.5 ppb in less than 5 minutes because of the fast interfacial reaction between the thiol groups on the SAMMS surface and mercury in solutions)
- it had high selectivity for mercury without significant interference from other abundant cations (such as Ca^{2+} and Na^{+}) and anions such as CN^{-}, CO_3^{2-}, Cl^{-}, SO_4^{2-} and PO_4^{3-} in wastewater with Kd up to 10^8 for mercury and reduced mercury concentration below 10 ppt in aqueous salt solutions because of its molecular recognition of the functional groups
- SAMMS bound effectively to mercuries in cationic and metallic forms and in complexes of chlorides and organics such as methylmercury
- it was effective for removing mercury from aqueous liquid wastes, pump oil wastes, and mercury vapor because of its proper mixture of hydrophobic moity and a hydrophilic end functional grou (a single treatment of the SRS tritiated pump oil wastes using SAMMS powders removed 91% of its mercury content.)
- the mercury-laden SAMMS passed U.S. Environmental Protection Agency (EPA) Toxicity Characteristic Leach Procedure (TCLP) tests because of the strong chemical binding between mercury and thiol groups and stable ceramic matrixes
- mercury-SAMMS was stable up to 150°C in air and 70°C in aqueous solutions and is also expected to have strong biological durability due to its proper pore size for preventing bacteria from forming methylating mercury
- no secondary wastes were generated during application and disposal because of the simple column type operation without resorting to any additional chemicals
- the SAMMS is regenerable, using concentrated hydrochloric acid if it is desired because of the ion exchangeable nature of thiol groups under strong acidic conditions
- SAMMS is also applicable in removing radionuclides (e.g., Pu, Np, and Am), anions ($H_2A_sO_4^{-}$, CrO_4^{2-}, ReO_4^{-}), and dense nonaqueous phase liquids (DNAPLs) because of its flexibility in

incorporating a range of functional groups

- preliminary cost estimates indicated lower life-cycle cost for applications of SAMMS in comparison with existing technologies because of simplicity in operation and manufacture and high waste loadings.

Glossary

SAMMS	self-assembled mercaptan on mesoporous silica
DOE	U.S. Department of Energy
UEFPC	Upper East Fork Poplar Creek
NPDES	National Pollution Discharge Emission Standard
EPA	U.S. Environmental Protection Agency
RCRA	Resource Conservation and Recovery Act
TEM	transmission electron microscopy
EDS	electron energy-dispersive spectroscopy
NMR	nuclear magnetic resonance
SP	single pulse
EXAFS	extended x-ray absorption fine structure
PNNL	Pacific Northwest National Laboratory
SRS	Savannah River Site
BET	Bruneau, Emmett, Taylor
SIAC	sulfur-impregnated activated carbon
TCLP	Toxicity Characteristic Leach Procedure
NRWTP	Nonradiological Wastewater Treatment Plant
DNAPL	dense nonaqueous phase liquids
MWFA	Mixed Waste Focus Area

Acknowledgments

This work is funded by the Efficient Separations and Processing Crosscutting Program, Office of Science and Technology of the U.S. Department of Energy. Financial support from Pacific Northwest National Laboratory (PNNL) through Laboratory Directed Research and Development (LDRD) funding on the basic science part of the research related to this project is also acknowledged. Pacific Northwest National Laboratory is operated for the U.S. Department of Energy by Battelle under Contract DE-AC06-76RLO 1830. The authors thank Tim Kent (Oak Ridge National Laboratory) for providing valuable information on the current system for mercury removal at the Nonradiological Wastewater Treatment Plant. The authors also thank Kriston Brooks and Larry Bagaasen for obtaining capital cost estimates for skid mounted and installed column systems, Mike Lilga for reviewing this report, Jim Buelt, Joe Perez, Nick Lombardo, Bill Kuhn, Jud Virden, Bill Bonner, Bruce Bunker, Rod Quinn, and John Sealock for consistent support of the development of this technology.

Contents

Figures

Tables

1.0 Introduction

Since they were discovered at Mobile Corporation five years ago (Beck et al. 1992; Kresge et al. 1992), mesoporous materials (Beck and Vartuli 1996; Liu et al. 1996; Huo et al. 1994; Maschmeyer et al. 1995; Tanev and Pinnavaia 1995; Bagshaw et al. 1995; Attard et al. 1995; Firouzi et al. 1995, Tianet al. 1997) have attracted considerable attention because of their high surface area of up to 1500 m^2/g and well defined pore size and pore shape. The great potential of these materials in environmental and industrial processes has not been fully realized because most of these applications, such as separation, catalysis, and sensing, require the materials to have specific functionality (Sayari 1996; Anthony et al. 1993; Schierbaum 1994). However, the self-assembled organic monolayers can provide a substrate with the dense surface functionality (Ball 1994) to enable its high selectivity for fine chemical control (Ulman et al. 1991), sensing (Kumar et al. 1994), and chemical separation (Wirth et al. 1997). The sensitivity of the sensors and the loading capacity of the separation resins made from these self-assembled organic monolayers are limited by the surface area available on the substrates.

We have recently developed a new class of materials (Feng et al. 1997b) by coating the mesoporous materials with functionalized organic monolayers, resulting in an efficient scavenger of mercury. This is an effective combination of the high selectivity of the self-assembled organic monolayers with the high surface area of the ordered mesoporous silica as shown in Figure 3.1. The self-assembled mercaptan on mesoporous silica (SAMMS) provides molecular recognition, and mesoporous silica provides an extremely high capacity for metal binding, resulting in a breakthrough material for separation.

This paper explains the technology that has been developed to produce SAMMS. It also discusses the characteristics of SAMMS materials and its application for mercury removal and stabilization. Finally, cost estimates are provided for producing SAMMS materials and its application for mercury removal from a wastewater.

2.0 Technology Needs

Chemical separations are particularly useful for environmental cleanup and remediation. Various industrial, military, agricultural, research, and hospital activities have resulted in severe contamination, especially metal contamination, in some areas. In these areas, metal contamination is present in air, in water, in sludge, in sediment, and in soil. Specifically, mercury appears in three primary forms:

1. metallic mercury: Hg^0
2. inorganic mercury: divalent mercury, Hg^{2+}; monovalent mercury, Hg_2^{2+}; neutral mercury compounds, $HgCl_2$, $Hg(OH)_2$
3. organic mercury: phenylmercury, $C_6H_5Hg^+$, $C_6H_5HgC_6H_5$; alkoxyalkyl mercury, $CH_3O\text{-}CH_2\text{-}CH_2\text{-}Hg^+$; methylmercury, CH_3Hg^+, CH_3HgCH_3.

These compounds can be ranked in order of decreasing toxicity as: methylmercury, mercury vapor, inorganic salts of mercury, and a number of organic forms, such as phenylmercury salts (Mitra 1986). Methylmercury, the most toxic form, is formed mainly by methylation of mercury by the methanogenic bacteria that are widely distributed in the sediments of ponds and in the sludge of sewage beds. In addition, methylation was used as a seed-dressing preparation in agriculture. Mercury poisoning in humans causes digestive disturbances, emaciation, diarrhea, speech stammering, delirium, paralysis of the arms and legs, and death by exhaustion.

The importance of mercury contamination is underscored by the fact that the U.S. Department of Energy (DOE) has identified the removal/separation/stabilization of mercury as the #1 and #4 priorities among 30 prioritized deficiencies. Over 50,000 m^3 of mixed low-level and transuranic waste-containing mercury has been identified in the DOE complex.. At the DOE Oak Ridge Site, an estimated 2.5 million pounds of mercury was lost to soil and surface water and 914 m^3 of mercury is contained in plant sumps. The headwaters of Upper East Fork Poplar Creek (UEFPC) are within the DOE Y-12 plant boundary, and 26,530,000 L of water per day are discharged to Lower East Fork Poplar Creek. The UEFPC is contaminated with low levels of mercury. A mercury-reduction program at the Oak Ridge Site has achieved point-source reduction, and mercury treatment systems are placed such that the mercury surface water concentration is declining. However, the program has not be able to meet the National Pollution Discharge Emission Standard (NPDES) permit that requires that treatment to 0.012 µg/L is needed at UEFPC by April 27, 2000. Exceeding the anticipated limit triggers the requirement of monitoring methyl mercury in edible portions of fish present in contaminated streams (UEFPC). If methyl mercury concentration exceeds 1 mg/kg, the public must be protected from ingestion of fish.

Many mercury-bearing DOE wastes are aqueous and non-aqueous liquids, sludges, soils, absorbed liquids, partially or fully stabilized sludges, and debris. Many wastes, including DOE wastes, contain mercury in amounts of less than 260 ppm; these wastes are not required to be treated by retorting as specified by the U.S. Environmental Protection Agency (EPA) regulation for mercury. However, these wastes contain other contaminants that require treatment, and the presence of mercury complicates the design of offgas systems, stabilization of residues, and monitoring of all effluents. It would be advantageous to remove the mercury as a pretreatment to simplify downstream operation.

Other metals that are of interest for remediation and other separations include, but are not limited to, silver, lead, cadmium, uranium, plutonium, neptunium, americium, and combinations thereof. Inorganic anions are also of interest for separations and include TcO_4^-, CrO_4^{-2}, AsO_4^{-3}.

The existing technologies for Resource Conservation and Recovery Act (RCRA) metal and mercury removal from diluted wastewater include sulfur-impregnated carbon (Otanl et al. 1988), microemulsion liquid membranes (Larson and Wiencek 1994), ion exchange (Ghazy 1995), and colloid precipitate flotation (Ritter and Bibler 1992). These different treatment methods have their own unique characteristics that provide advantages for certain specific applications. In the sulfur-impregnated carbon process, metal is adsorbed to the carbon, not covalently bound to the matrix as with SAMMS. The carbon materials are inexpensive and also adsorb organics in addition to RCRA metals. The adsorbed metal may need secondary stabilization because the metal-laden carbon may not have the desired long-term chemical durability because of the weak bonding between metal and active carbons. In addition, a large portion of the pores in the active carbon is large enough for the entry of microbes to solubilize the mercury-sulfur compounds. The RCRA metal loading is not as high as that of mesoporous-based materials. The microemulsion liquid-membrane technique uses an oleic acid microemulsion liquid membrane containing sulfuric acid as the internal phase to reduce the wastewater mercury concentration effectively from 460 ppm to 0.84 ppm (Larson and Wiencek 1994). This process involves multiple steps of extraction, stripping, demulsification, and recovery of mercury by electrolysis with the use of large volumes of organic solvents. The liquid membrane swelling has a negative impact on extraction efficiency. The slow kinetics of the RCRA metal-ion exchanger reaction requires long contact time. This process may also generate large volumes of organic secondary wastes. The ion exchange process (Ghazy 1995) uses Duolite™ GT-73 ion exchange organic resin to reduce the mercury level in wastewater from 2 ppm to be below 10 ppb. The mercury loading was limited to about 0.145 g/mL due to low surface area. In addition, the mercury-laden organic resin may not have the ability to resist microbe attack, and mercury may be released into the environment if it is disposed of as a long-term waste form. The reported successful removal of RCRA metal from water by colloid precipitate flotation reduces mercury concentration from 160 ppb to about 1.6 ppb [8], which can address many of the remediation needs. This process involves the addition of HCl to adjust the wastewater to pH 1, the addition of Na_2S and oleic acid solutions to wastewater, and the removal of colloids from the wastewater. In this process, the treated wastewater is potentially contaminated with the Na_2S, oleic acid, and HCl by the treatment itself. The separated mercury needs further treatment to be stabilized as a permanent waste form for disposal.

No effective existing technologies have been developed for removing mercury from organic media such as pump oil. Some preliminary laboratory study of a zinc powder/filtration process was carried out by the Pantex Plant with certain success, but the work was discontinued[(a)].

Thus, there remains a need for materials and methods for separations that have high selectivity and high capacity and do not require secondary treatment. There remains a need for separations of hazardous metals in complex compounds. More specifically, there remains a need for material that can reduce mercury concentration in groundwater to below 0.012 µg/L and works in organic liquids such as pump oils as well as in used organic solvents.

(a) Klein JE. "R&D Needs for Mixed Waste Tritium Pump Oils (U)," Westinghouse Savannah River Company Inter-Office Memorandum, SRT-HTS-94-0235, July 11, 1994.

3.0 Technology Description

The SAMMS materials are based on self-assembly of functionalized monolayers on mesoporous oxide surfaces (Feng et al. 1997b). Figure 3.1c shows a schematic drawing of the SAMMS material that is a combination of the self-assembled functional monolayers (Figure 3.1a) and mesoporous oxides (Figure 3.1b showing a transmission electron microscopy [TEM] micrograph of the mesoporous silica).

3.1. High Surface Mesoporous Supports

The unique mesoporus oxide supports provide high surface area (>1000 m^2/g), thereby enhancing the metal-loading capacity. They also provide an extremely narrow pore-size distribution, which can be specifically tailored from 15 Å to 200 Å, thereby minimizing biodegradation from microbes and bacteria (>20,000 Å). Mesoporous structures may be disposed of as stable waste forms.

Mesoporous silica materials were synthesized in cetyltrimethylammonium chloride/hydroxide, silicate, and mesitylene solutions (Beck et al. 1992). Typically, cetyltrimethylammonium chloride/hydroxide (CTAC/OH) solution was prepared by batch contact of 29 wt% CTAC (Carsoquat CT-429, Lonza, Inc.) with strongly basic ion exchange resin (DOWEX-1, Sigma Chemical Co., 0.2 g resin/g 29 wt% CTAC solution), 13 g colloidal silica (Hi-Sil 233, PPG Industries), 51 g tetramethylammonium silicate (10% SiO_2, 0.5 TMA/Si mole ratio, SACHEM, Inc.), and 28 g mesitylene (Eastman Kodak) were added in that order to each 100 g CTAC/OH solution. The mixture was sealed in a Teflon-lined vessel and heated at 105°C for 1 week. The product was recovered by suction filtration, dried at ambient temperature, and calcined at 540°C for 1 h in flowing nitrogen, followed by 12 h in flowing air. The calcined mesoporous silica has a surface area of 900 m^2/g and an average pore size of 55 Å, as determined by the gas adsorption technique using an AUTOSORB DEGASSER, QUANTACHROME, and TEM.

3.2. Self-Assembled Functional Groups on Mesoporous Oxide Surfaces

The self-assembled functional group provides three important functions: 1) molecular recognition for metals, 2) covalent bonding to the support materials, and 3) high population density of the functional groups on the substrate surfaces.

Molecular self-assembly is a unique phenomenon in which functional molecules aggregate on an active surface, resulting in an organized assembly with both order and orientation (Fryxell et al. 1996; Bunker et al. 1993; Tarasevich et al. 1996). In this approach, bifunctional molecules containing a hydrophilic head group and a hydrophobic tail group adsorb onto a substrate or an interface as closely packed monolayers. The driving forces for the self-assembly are the inter- and intra-molecular interactions between the functional molecules. The tail group and the head group can be chemically modified to contain certain functional groups to promote covalent bonding between the functional organic molecules and the substrate on one end, and the molecular bonding between the organic molecules and the metals on the other. By populating the outer interface with functional groups, an effective means for scavenging heavy metals is made available.

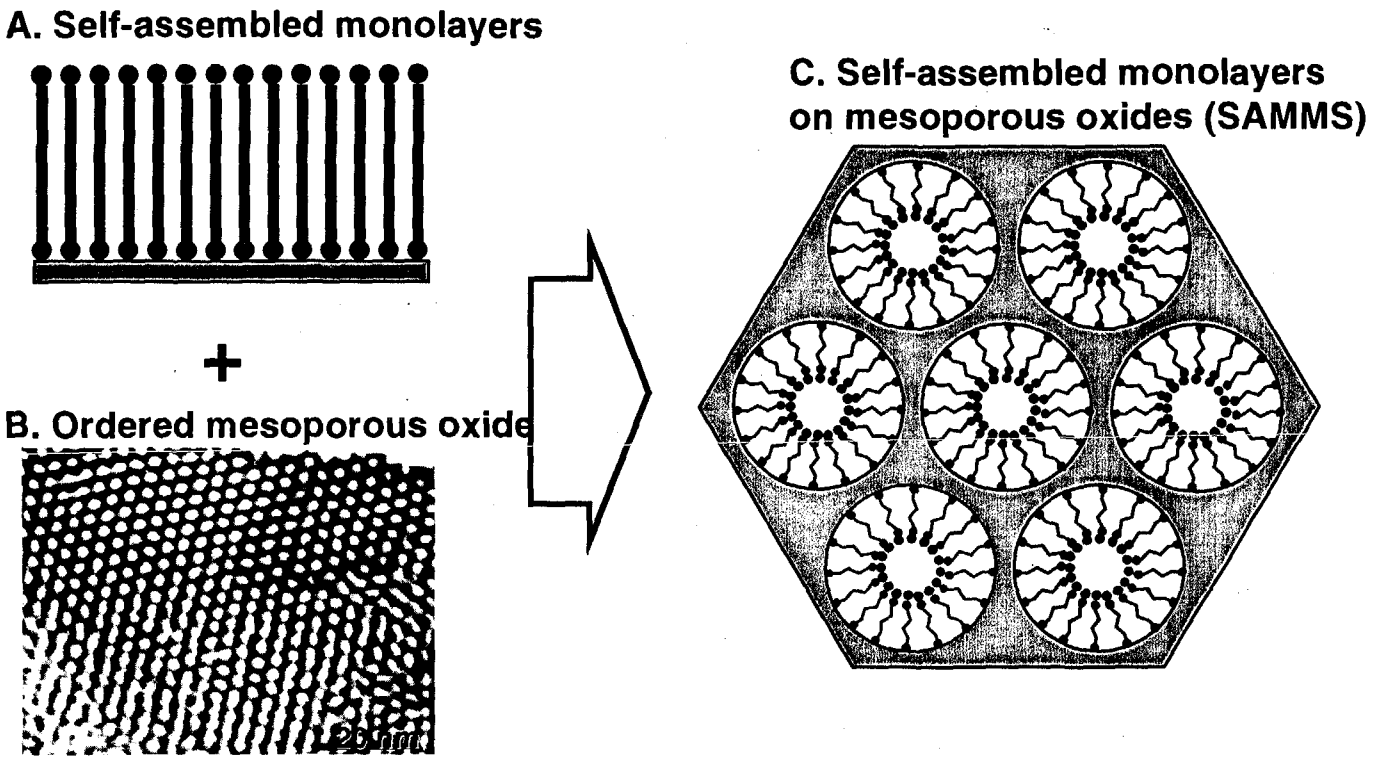

Figure 1. (A) A schematic representation of self-assembled functional monolayers
(B) TEM micrograph of mesoporous silica, showing uniform and ordered porosity
(C) A schematic representation of SAMMS materials, which is a result of A + B.

Functional groups (thiol groups in this case) were introduced to the pore surface of mesoporous silica as the terminal groups of organic monolayers. The hydrocarbon chains aggregate and form close-packed arrays on the substrate. The siloxane groups then undergo hydrolysis and ultimately end up covalently attached to the substrate and crosslinked to one another, resulting in the novel material, called SAMMS.

The population density and the quality of the functionalized monolayers on the mesoporous materials are greatly affected by two factors: the population of silanol groups and adsorbed water molecules on the mesoporous silica surface. The silanols anchor the organic molecules to the silica surface. However, the calcining step used in preparing mesoporous silica dehydrates the silica surface and removes most of the silanols, which results in poor surface coverage (Gao and Reven 1995). A proper amount of adsorbed surface water is also important because the hydrolysis reaction is one of the critical first steps in the process of building the monolayer. Ideally, just enough water would be associated with the surface for the siloxane hydrolysis. The existence of free water is detrimental to the efficient formation of a clean monolayer because of polymerization of tris(methoxy)mercaptopropylsilane (TMMPS) in solution (Tripp and Hair 1992).

The initial strategy was to rehydrate the mesoporous silica surface. This process involved boiling a weighed sample of mesoporous silica in pure water for several hours, collecting the silica by filtration, weighing it again, and removing the surplus water content via azeotropic distillation with toluene. This method, although successful in the deposition of high quality monolayers up to 75% surface coverage, was time-consuming and laborious. Recently, we have developed a more efficient approach by wetting the silica surface with 2 to 2.5 monolayers of water (based on available surface area). Experimentally, this approach is accomplished by adding the requisite amount of water to a suspension of mesoporous silica in toluene and stirring the mixture for an hour to allow complete dispersal of the aqueous phase across the ceramic interface. When the mesoporous ceramic interface is properly hydrated, the monolayer is constructed by adding one equivalent (or a slight excess) of the desired alkoxysilane (based on available surface area), stirring the mixture, and heating it in toluene reflux for several hours. Currently, we can systematically vary the population densities of functional groups on the mesoporous materials from 10% up to 100% of the full surface coverage.

The relative surface coverage was estimated based on 1) the surface area of the support, 2) the weight change after the functionalized monolayers were attached, and 3) the ideal loading density that can be achieved on flat surfaces. These results were also verified by electron energy-dispersive spectroscopy (EDS). We systematically varied the population densities of functional groups on the mesoporous materials from 10 to 100% of the full surface coverage.

The population density of organic monolayers for 100% coverage on silica was determined using ^{13}C solid state nuclear magnetic resonance (NMR) methods on dense fumed silica spheres with a known surface area (150 m^2/g) and tetrakis(trimethylsilyl)silane $(TMS)_4Si$ as an internal standard. Integration of the peaks from functionalized monolayers and from the internal standard allowed the determination of the number of alkylsiloxanes on the substrate.

3.3. Molecular Structure and Chemical Bonding of SAMMS Materials

The structure of the functionalized monolayers and the chemical bonding can be studied by solid-state NMR experiments (Wang et al. 1996; Badia et al. 1996). The 75.0 MHZ ^{13}C solid-state NMR experiments were carried out with a Chemagnetics spectrometer (300 MHZ - 89-mm wide-bore Oxford magnet) using a double-resonance probe. For both unloaded and mercury-loaded SAMMS samples, single-pulse (SP) Bloch-decay and cross-polarization (CP) methods were used with ^{1}H decoupling. The dried powders were loaded into 7-mm Zirconia PENCILTM rotors and spun at 3 to 4 kHz. Spectra were collected by using an SP excitation Bloch-decay method with a 5-μs (90°) ^{13}C pulse and a 10-s repetition delay. For all experiments, 40-ms acquisition times and a 50-KHz spectral window were employed. The number of transients was 1000 to 3000. The power levels of the carbon and proton channels were set so that the Hartmann-Hahn match was achieved at 55 kHz in CP experiments with 3-ms contact time and 5-s repetition delay. A Lorentzian line broadening of 24 Hz was used for all ^{13}C spectra. The 59.3 MHZ ^{29}Si NMR spectra were also taken for both samples using the SP Bloch-decay method with ^{1}H decoupling. A Lorentzian line broadening of 50 Hz and a 30-s repetition delay were used for ^{29}Si spectra. Both ^{13}C and ^{29}Si NMR chemical shifts were referenced to TMS at 0 ppm.

Single-pulse ^{13}C NMR spectra along with the peak assignments {Si-CH2(3)-CH2(2)-CH2(1)-SH} for 25%, 76%, and mercury-laden 76% functionalized monolayers samples, respectively, are shown in Figure 3.2. For 25% functionalized monolayers coverage on mesoporous silicates (Figure 3.2A), the peak at 12.8 ppm was attributed to the methylene carbon group C3, directly bonded to the Si atom. The peak at 28.3 ppm was attributed to the other two methylene carbons (C2 and C1). An additional peak at 24.7 ppm (Figure 3.2B) was observed for 76% functionalized monolayers coverage. This peak was assigned to the methylene carbon (C1) next to the -SH group, based on the chemical shifts reported for $CH_3(CH_2)_7SH$ (Wang et al. 1996; Badia 1996).

The difference in Figure 3.2A and Figure 3.2B is attributed to a different molecular conformation for the organic monolayers at different coverages. At low surface coverage, the carbon chains can adapt a wide range of conformations; therefore, the peaks for C2 and C1 cannot be distinguished because of conformational heterogeneity. At higher population densities, all of the carbon chains are near one another and have a more upright orientation with respect to the silica surface. The molecules have a higher degree of ordering that narrows the linewidths in the ^{13}C spectrum and allows the peaks for all three carbons to be resolved better. The close-packed conformation of the carbon chains is also evident in ^{29}Si NMR results (Figure 3.3). It is important to recognize that relative peak intensities in ^{29}Si CP-MAS are not strictly quantifiable because of differences in relaxation behavior. Therefore, we have used the Bloch decay pulse sequence (single-pulse excitation) with long recycle times to obtain data that allow us to quantify the molecular composition of these materials. The large peak at -111 ppm is from the silica support. In Figure 3.3A, three additional peaks from -50 to -80 ppm are identified for the 25% functionalized monolayers coverage, corresponding to three different environments for the siloxane groups in the functionalized monolayers (Sindorf 1983): 1) isolated groups that are not bound to any neighboring siloxanes, 2) terminal groups that are only bound to one neighboring siloxane, and 3) cross-linked groups that are bound to two neighboring siloxanes. Among the three, the most dominant peak comes from terminal group (2). For 76% functionalized monolayers coverage, the molecules are closer to one another, and the most predominant peak corresponds to the cross-linked siloxane group (3). The isolated siloxane group (1) is absent. The transition from disordered conformation at low surface coverage to close-packed conformation at high coverage is illustrated in Figure 3.4.

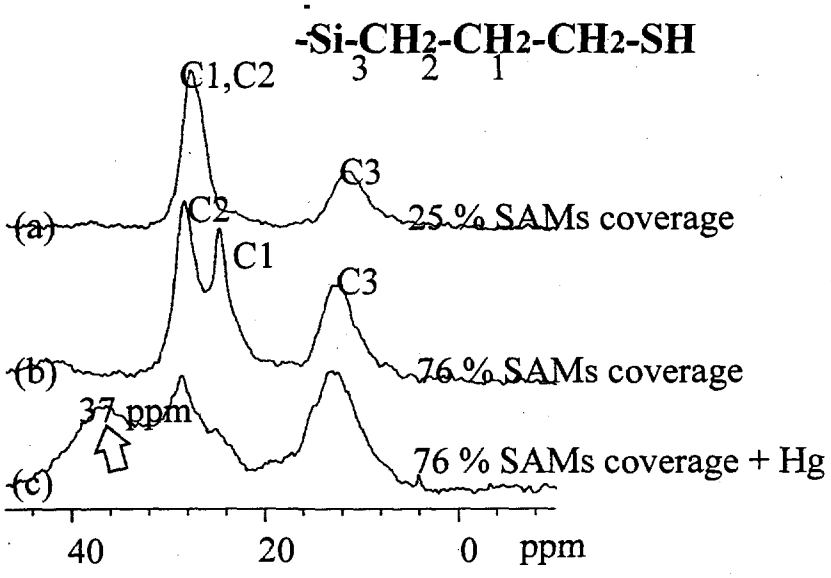

Figure 3.2. ^{13}C NMR spectra of monolayers of mercaptan on mesoporous silica: (A) At 25% coverage; (B) at 76% coverage; (C) at 76% coverage with Hg

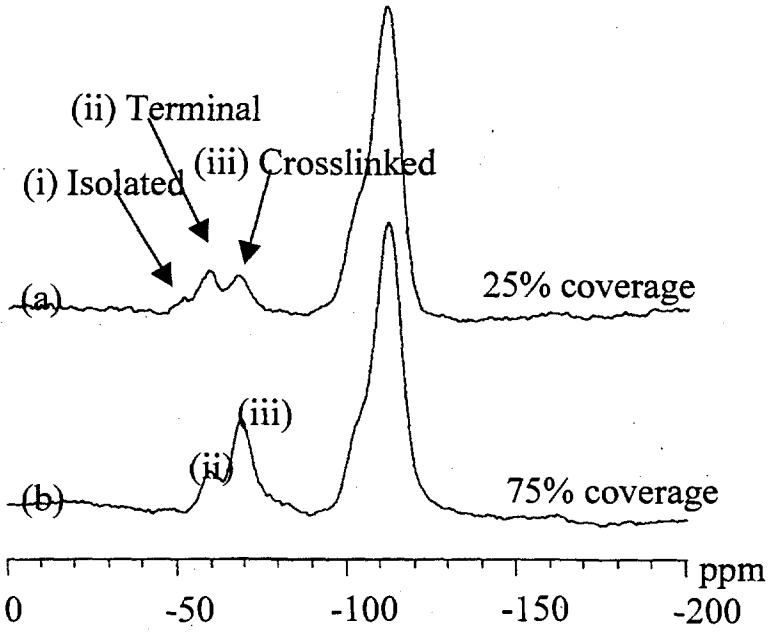

Figure 3.3. ^{29}Si NMR spectra of SAMMS with (A) at 25% and (B) 76% surface coverage

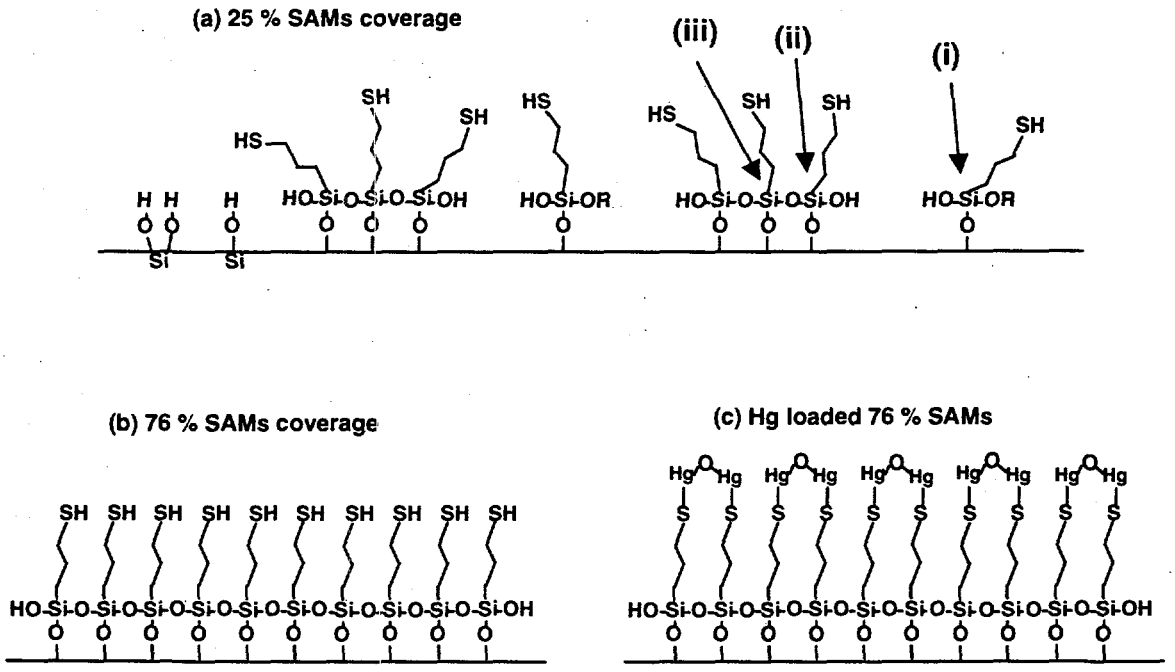

Figure 3.4. Schematic conformations of monolayers with different coverage. (A) Disordered molecule at 25% coverage; (B) Close-packed at 76% coverage; (C) Bound to Hg at 76% coverage.

The ^{13}C spectrum for the 76% functionalized monolayers coverage with mercury (Figure 3.2C) shows that the three resonances corresponding to the C1, C2, and C3 methylene carbons observed in Figure 3.2B are still discernible, but become much broader. A new broad peak appears at 37 ppm, and the peak at 24.7 ppm decreases significantly. This result suggests strong chemical bonding between the mercury and thiol group, which causes the shift of the peak corresponding to C1 attached to the thiol group. The next C2 group is also affected, but to a lesser degree. The fact that the peak at 24.7 ppm is still present indicates that the thiol groups are not saturated with mercury yet.

The SAMMS material is a useful environmental remediation agent because it has a high affinity for binding mercury and other heavy metals. Figure 3.1B is a TEM micrograph of SAMMS with 76% coverage after contact with a solution containing mercury ions. The ordered porous structures were preserved in the chemical treatment processes for attaching the functionalized monolayers. Although most mercury was evaporated under the electron beam and therefore was not visible in the TEM image, some mercury was detected in the EDS spectrum (Figure 3.5). The EDS also detected sulfur from the thiol group. Compositional analysis indicates that the relative concentration for sulfur and silica is 5.2 mmol/g of silica, which is in excellent agreement with the gravimetric estimate (5.6 mmol/g).

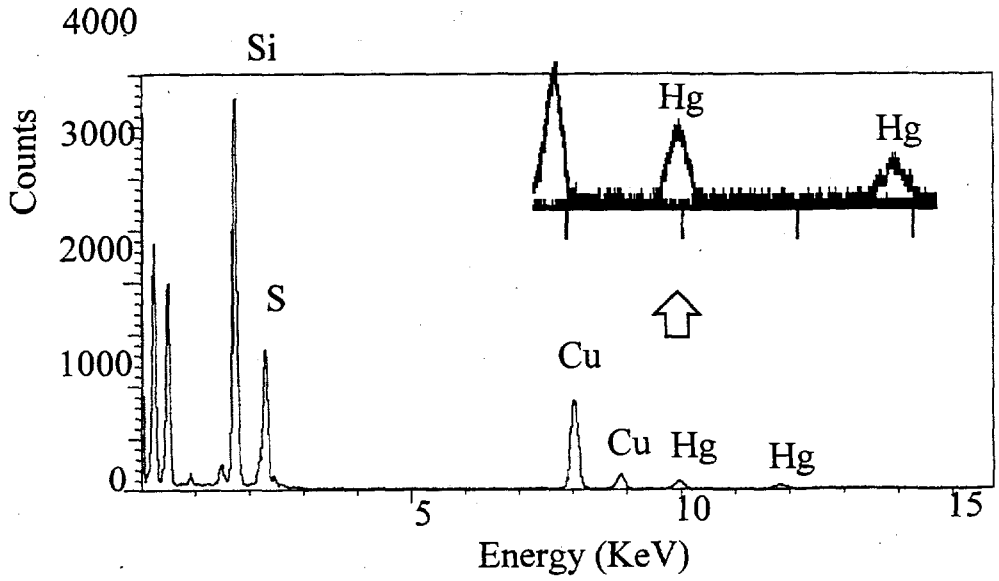

Figure 3. 5. EDS spectra of Hg-SAMMS

The chemical bonding between mercury and the thiol group was further confirmed by extended x-ray absorption fine structure (EXAFS) studies. EXAFS experiments on the mercury-laden SAMMS were performed at the m mercury L_{III} absorption edge on beamline X18B at the National Synchrotron Light Source at Brookhaven National Laboratory. Measurements of tape mounts of mercury sulfide and mercury oxide standards were made in the transmission mode. SAMMS samples were measured in the fluorescence mode, utilizing the Stern/Heald configuration while simultaneously monitoring the absorption signal of the mercury sulfide reference on the downside of the experiment to allow investigation of the valence state of mercury in the sample. Data were reduced and analyzed according to recommended procedures (Stern and Heald 1979; Sayers and Bunker 1988). The National Synchrotron Light Source is supported by the U. S. Department of Energy, Office of Energy Research, Division of Materials Sciences and Division of Chemical Sciences.

A schematic of the proposed structure is illustrated in Figure 3.4C. When the mercury binds to the thiol group, the mercury-S and mercury-O bond lengths are 2.4 $\pm$ 0.01Å and 2.14 $\pm$ 0.01Å, respectively. The mercury atoms on the two adjacent thiol groups are linked by the same oxygen atom with a mercury-mercury separation of 3.99 $\pm$ 0.05 Å, and the bond angle of mercury-O-mercury is calculated to be 137°.

4.0 Characteristics of SAMMS Materials

The SAMMS materials used for this study were from two batches of synthesized materials at Pacific Northwest National Laboratory (PNNL). The first batch of materials, labeled as SAMMS #1, has about 25% surface coverage with functional groups; the second batch of the materials (SAMMS #2) has a functional group coverage of over 80% of its surface. The mercury analysis was performed using a CETAC M-6000A Mercury Analyzer System with a detection limit of 10 ppt.

4.1 Physical Characteristics

The materials are white powders with a particle size ranging from 5 to 15μm; the pore size within the particles is about 5 nm. The surface area measured 871 m^2/g. The measurements of the BET surface area and the pore size were conducted using an Autosorb Degasser (Quantachrome). One of the best commercial mercury absorbers, Duolite GT-73 (referred as GT-73), manufactured by Rohm and Haas Company, was used in this study for comparison with SAMMS, and GT-73 is in the form of polymer beads with a size of over 300 μm.

4.2 Mercury Loading

4.2.1 Sorption Isotherm Experiment

In this experiment, $NaNO_3$ was added to give a 0.1 M of Na^+ concentration to ensure a rigorous test of selectivity. In the experiment, a 10-mg sample of SAMMS #2 was added to 50-mL polypropylene centrifuge tubes containing variable amounts of 0.1 M $NaNO_3$ solution. An aliquot containing a different amount of 0.1 M $Hg(NO_3)_2$ was added to each centrifuge tube containing the SAMMS #2 to obtain initial mercury concentrations of 0 to $2.0 \cdot 10^{-3}$ mg/L. The final volume of the solutions in each test was 50 mL. The slurries were then shaken for 4 hours to reach equilibrium (see Section 4.3) before they were filtered. The filtrates were analyzed for pH and total mercury. The test at each mercury concentration was conducted in triplicate, and the sorption isotherm experiment was also performed using $HgCl_2$.

The equilibrium mercury-loading capacity depends on the mercury concentrations in the liquid phase. Figure 4.1 illustrates the loading capacities of SAMMS #2 in 0.1 M $NaNO_3$ solutions containing different amounts of mercury. The equilibrium capacities changed from 83 mg/g at 0.24 ppb of mercury to 635 mg/g at 670 ppm of mercury in the form of Hg^{2+} (Figure 4.1a and Table 4.1). The loading capacity for $HgCl_2$ (Figure 4.1b and Table 4.2) is slightly lower than that for $Hg(NO_3)_2$. For instance, the loadings for $HgCl_2$ at a mercury concentration of 171 ppm is 500 mg/g. Mercury loading for $Hg(NO_3)_2$ is 610 mg/g at the same mercury concentration. The mercury-loading capacity in pump oil was measured only on SAMMS #1 with a value of 1.2 mg/g at a mercury concentration of 0.635 ppm.

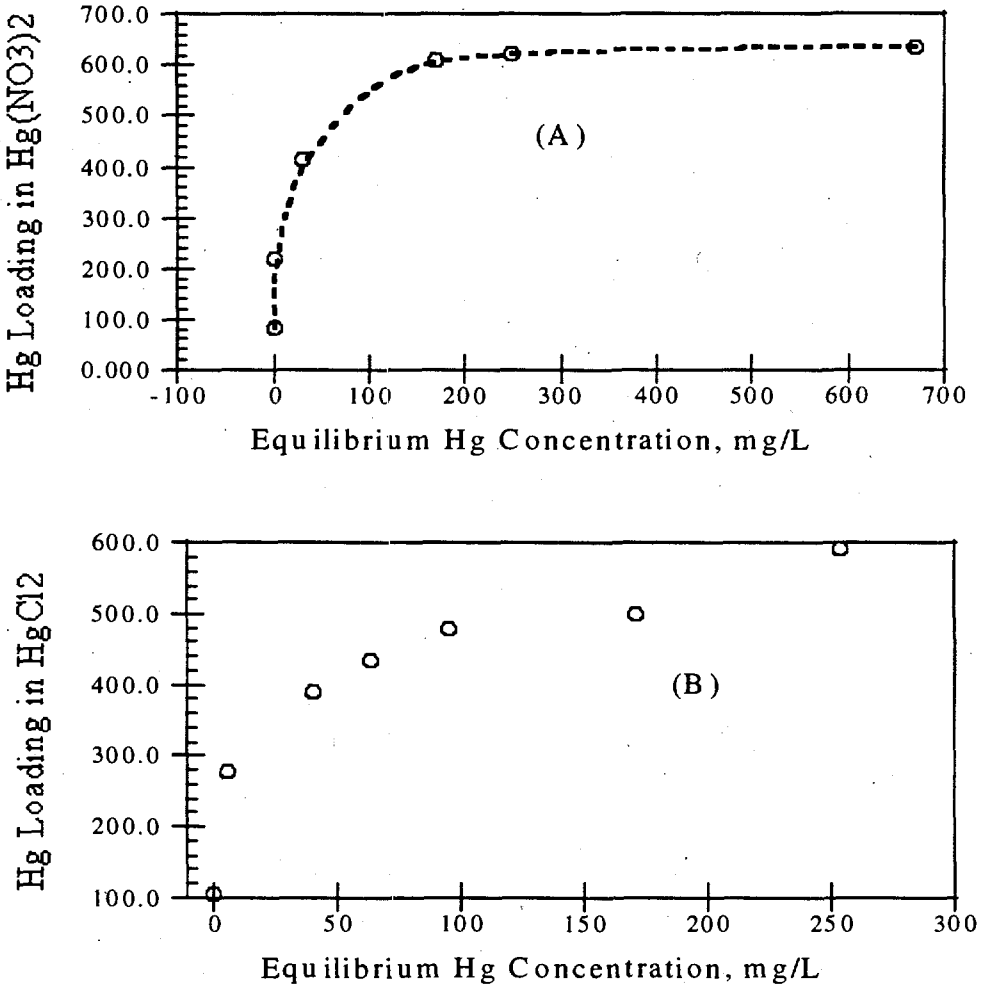

Figure 4.1. Equilibrium Mercury Loading of SAMMS #2: (A) for Hg^{2}+; (B) for $HgCl_2$

Table 4.1. Equilibrium Mercury Loading in $Hg(NO_3)_2$ Solutions

SAMMS	pH_{Ini}	pH_{Fin}	Hg Conc. mg/L	Loading, mg Hg/g	In Liquids
#2	NA	NA	0.00024	83.00	0.1 M $NaNO_3$
#2	3.43	3.35	1.3	218	0.1 M $NaNO_3$
#2	3.28	3.08	30	415	0.1 M $NaNO_3$
#2	2.98	2.81	170	610	0.1 M $NaNO_3$
#2	2.90	2.73	250	621	0.1 M $NaNO_3$
#2	NA	NA	670	635	0.1 M $NaNO_3$
#1*	NA	NA	0.635	1.2	pump oil
#1*	NA	NA	0.066	0.24	pump oil

* The contact time of SAMMS #1 with pump oils was limited to two hours at room temperature; these data may not represent equilibrium data. NA=Not Available

Table 4.2. Equilibrium Mercury Loadings in $HgCl_2$ Solutions

SAMMS	pH_{Ini}	pH_{Fin}	Hg Conc. mg/L	Loading, mg Hg/g	Kd
#2	4.06	3.73	0.00	105.00	1.E+08
#2	3.63	3.33	6.00	277.00	46083
#2	3.35	3.10	40.67	389.00	9570
#2	3.22	3.01	63.70	434.00	6813
#2	3.12	2.95	95.10	480.00	5042
#2	2.94	2.83	171.00	500.00	2924
#2	2.83	2.73	254.00	593.00	2336

The mercury absorption in 0.1 M $NaNO_3$ solutions exhibited a Langmuri isotherm curve (Figure 4.1a) and showed an excellent fit ($R^2 = 0.999$) to the Langmuri isotherm equation (Figure 4.2a), which follows the general form:

$$\frac{C}{Q} = \frac{1}{K} + \frac{C}{b} \tag{1}$$

where C is the equilibrium concentration of mercury (mg/L), Q is the mercury equilibrium loading on SAMMS (mg/g), K is the Langmuri adsorption constant (g/L), and b is the maximum amount of mercury that can be bound by SAMMS (mg/L). Fitting by least-square yields a value for K of 61.4 g/L and a value for b of 650 mg/L.

The perfect fit to a Langmuri Isotherm curve may suggest a monolayer adsorption of mercury on the SAMMS surface, which is consistent with the molecular structure shown in Figure 3.4 with SAMMS over 76% surface coverage as derived from the NMR and EXAFS study discussed in Section 3.3. The maximum loading of 650 mg/L determined from the Langmuri Isothermo equation (4.1) is also consistent with the observed maximum loading of 635 mg/L.

4.3 Binding Kinetics

4.3.1 Kinetic Experiments

The experiments involved two total mercury concentrations of ~0.5 and 10 mg/L in 0.1 M $NaNO_3$. A total of 0.24 g of SAMMS #2 or Duolite GT-73 was weighed into 500-mL bottles. In each test, 500 mL of the mercury solution was used. The solution to SAMMS ratio was approximately 2080 mL/g in each test. The bottles containing these slurries were shaken at room temperature for 8 hours. From each bottle, a 10-mL aliquot of the well-mixed slurry was collected at time intervals of 5, 10, 30, 60, 180, 360, and 480 minutes, and the aliquots were filtered immediately using a 10-mL plastic syringe mounted on a filter holder containing a 0.2-μm membrane filter. The filtrates were analyzed for total mercury concentration. A set of mercury solutions without the addition of any SAMMS was also treated in the same way as the SAMMS solutions to serve as blanks.

For a 500-ppb mercury solution (Figure 4.3a), SAMMS, at a solution-to-SAMMS ratio of 2080, reduced its concentration to 0.5 ppb within 5 minutes, and reduced to 10 ppt within 6 hours.

Figure 4.3b shows that SAMMS, at a solution-to-SAMMS ratio of 2080, reduced the 10-ppm mercury concentration to 3.1 ppb within 5 minutes, to 1.6 ppb in 10 minutes, and then stabilized at about 1.2 ppb. The corresponding behavior of the commercial mercury absorber, GT-73, also is shown in Figure 4.3. The curves in Figure 4.3a have not indicated an equilibrium (the 10-ppt detection limits of mercury analysis limited our ability to see concentration difference netween the last two data points for SAMMS), especially for GT-73. A longer test duration, such as 24 hours, may be needed for future study.

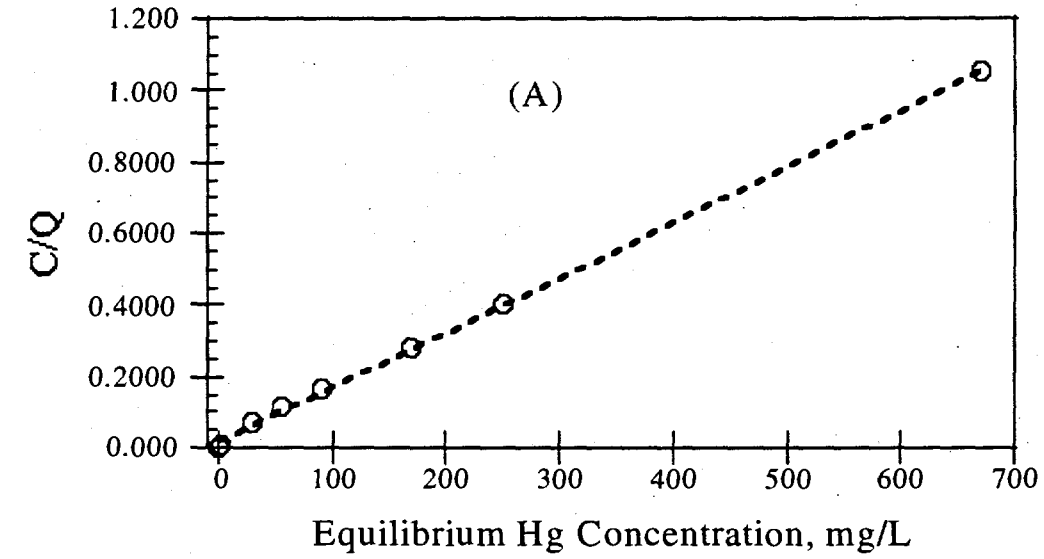

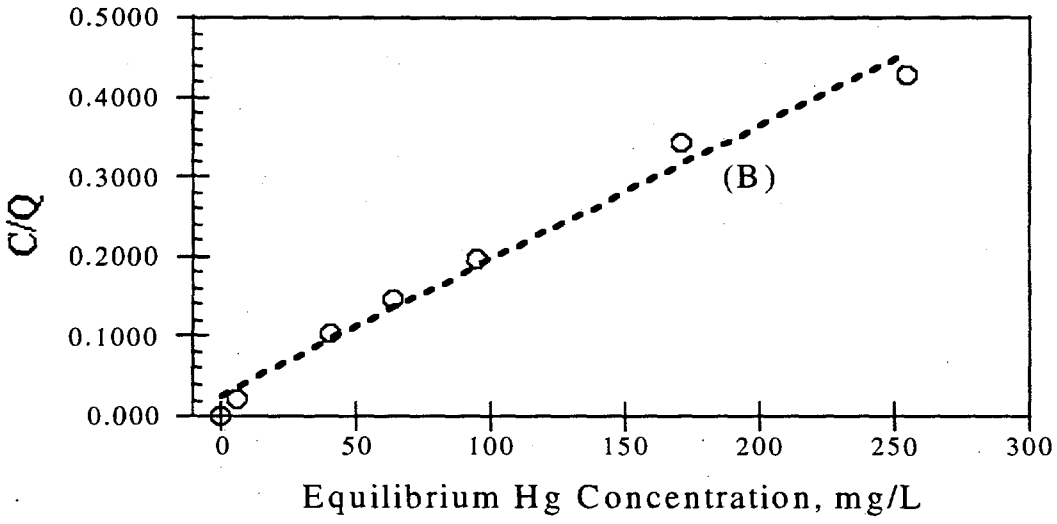

Figure 4.2. Langmur Isotherm Fitting of SAMMS#2: (A) Hg^{2}+; (B) for $HgCl_2$

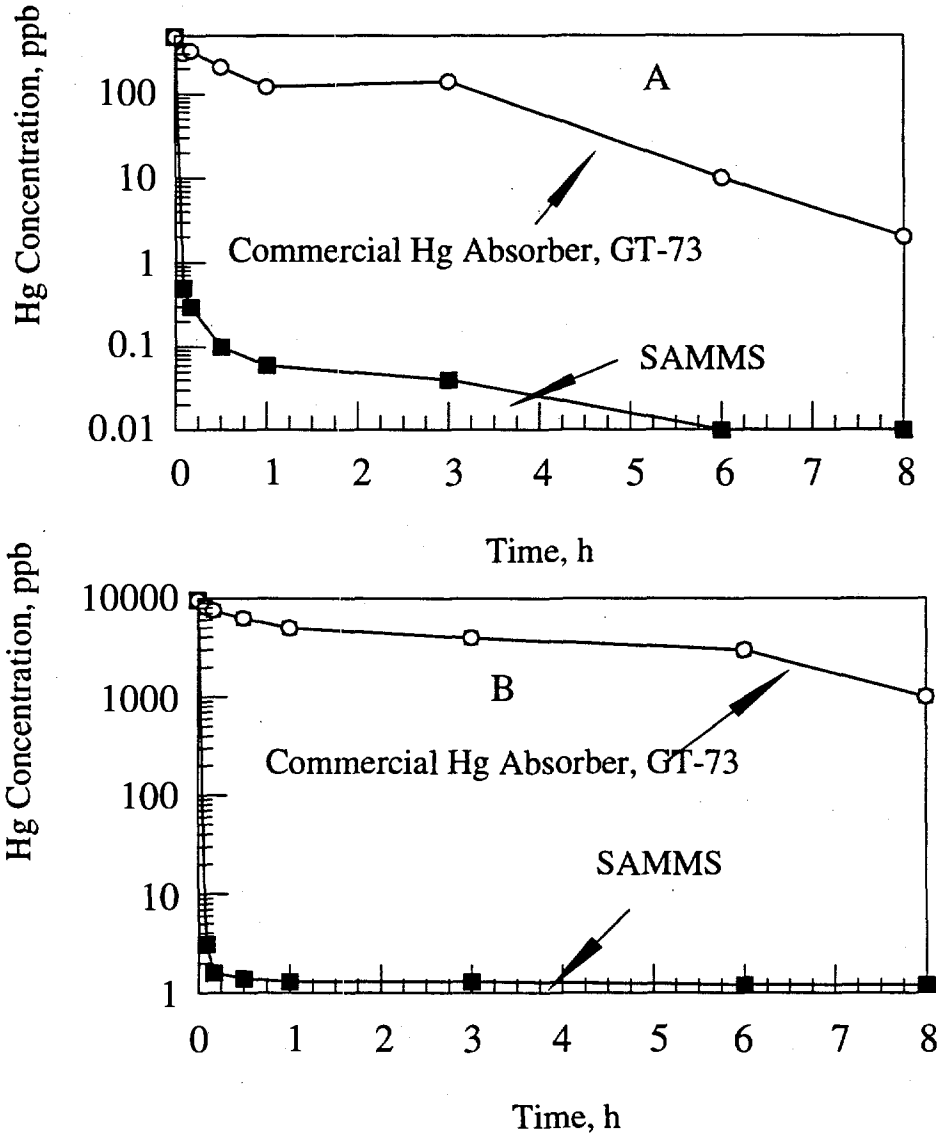

Figure 4.3. SAMMS Mercury Binding Kinetics: (A) in 500 ppn Mercury solution; (B) in 10.0 ppm Mercury Solution

From the practical point of view, the mercury binding of SAMMS is fast, and the current data yielded a near-zero time dependance of the binding kinetics. Shorter time durations are needed to derive the binding kinetics of SAMMS within the first 5 minutes of contact with mercury solutions.

Table 4.3 shows that the mercury distribution coefficient, Kd, values are up to 10^8 in aqueous solutions containing 0.1 M $NaNO_3$. The Kd was calculated through the concentration differences before and after mercury binding to SAMMS and the amount of mercury bound to SAMMS as follows:

$$Kd = \frac{(C_0 - C)V}{Cm} \qquad (2)$$

where

C_0 = initial mercury concentration in μg/mL
C = mercury concentration after contacting the solution with SAMMS in μg/mL
V = volume of the mercury solution that is in contact with SAMMS in mL
m = dry mass of the SAMMS used in g

Table 4.3. SAMMS #2 Mercury Binding Kd Values as a Function of Mercury Concentrations

Initial Hg, mg/L	Final Hg, mg/L	Hg solution, mL	SAMMS #2, g	Kd
0.487	0.00	500.00	0.24	$1.01 \cdot 10^8$
9.70	0.0012	500.00	0.24	$1.68 \cdot 10^7$
974	669	500.00	0.24	950.00

Kd values are a function of intial mercury concentration, solution volume, mass of absorbents, and the detection limit. The Kd value in Table 4.3 could be higher than $1.01 \cdot 10^8$ if the ercury detection limit were lower than 10 ppt.

4.4. Binding Speciations

The discussion in the *Introduction Section* showed that mercury contamination involves multiple speciations of mercury. To test the ability of SAMMS in binding to many different speciations of mercury, SAMMS was tested with cationic ions Hg^{2+}, complex $HgCl_2$, organic CH_3-Hg-OH, and metallic mercury.

Binding to cationic Hg^{2+}, and complex $HgCl_2$: The data in Sections 4.2 and 4.3 showed that SAMMS bonds effectively to cationic Hg^{2+} and complex $HgCl_2$. In solutions with pH higher than 4, the possible mercury speciations are $Hg(OH)_2$ and $Hg(OH)^+$ according to Baes and Mesmer (Baes 1976). The $Hg(OH)^+$ species in a $Hg(NO_3)_2$ solution may be the main contributor to the rection with SAMMS through the following binding reactions:

$$Hg(OH)^{+} + H\text{-}S\text{-}SAMMS = HO\text{-}Hg\text{-}S\text{-}SAMMS + H^{+} \quad (3)$$

$$MMS\text{-}S\text{-}Hg\text{-}OH + HO\text{-}Hg\text{-}S\text{-}SAMMS = SAMMS\text{-}S\text{-}Hg\text{-}O\text{-}Hg\text{-}S\text{-}SAMMS + H_2O \quad (4)$$

The above reactions are consistent with the observed pH (Table 4.1) decreasing due to the release of hydronium ions in Reaction (3) while $Hg(OH)_2$ reacting with HS-SAMMS does not result in a change of pH since only neutral H_2O is reduced in the reaction. The final products with an oxo bridge (Hg-O-Hg) formation on the surface of SAMMS shown in Reaction (4) are in agreement with the EXAFS measurements discussed in Section 3.3. In a $HgCl_2$ solution containing 0.1 m $NaNO_3$, there is the following equilibria:

$$HgCl_2 + H_2O = Hg(OH)Cl + H^{+} + Cl^{-} \quad (5)$$

$$HgCl_2 + H_2O = Hg(OH)^{+} + H^{+} + 2Cl^{-} \quad (6)$$

The $Hg(OH)^{+}$ species formed in Reaction (6) effectively binds to SAMMS through Reactions (3) and (4) as discussed above because we observed similar pH decreasing after SAMMS bound to mercury as in $Hg(NO_3)_2$ solutions. The Hg(OH)Cl species may also react with SAMMS through

$$Hg(OH)Cl + H\text{-}S\text{-}SAMMS = HO\text{-}Hg\text{-}S\text{-}SAMMS + H^{+} + Cl^{-} \quad (7)$$

$$Hg(OH)Cl + H\text{-}S\text{-}SAMMS = Cl\text{-}Hg\text{-}S\text{-}SAMMS + H_2O \quad (8)$$

Reaction (7) resulted in the same product of that in Reaction (3) and is also consistent with the observed solution pH decrease shown in Table 4.2. The mercury binding in $HgCl_2$ also showed a good Langmur Isotherm behavior (Figure 4.2b) with a least squre fitting of $R^2 = 0.9821$, k = 41.3 g/L, and b=588 mg/g. Reaction (8) can be ruled out because of the inconsistency with the observed solution pH decreasing, although Hg(OH)Cl is the major species in the solution (Baes 1976). The different products on the SAMMS surface may be futher verified through surface studies using NMR and EXAFS.

Binding to Organic Mercury: Methylmercury, the most toxic form, is formed mainly by methylation of mercury by the methanogenic bacteria that are widely distributed in the sediments of ponds and in the sludge of sewage beds. Methylmercury can accumulate in fish in contaminated waterways. Mercury poisoning symptoms in humans includes digestion disturbances, emaciation, diarea, speech stammering, delirium, paralysis of the arms and legs, and death by exhaustion. The recently reported tragic death of a university researcher who was using methylmercury is a graphic illustration of the toxicity of this compound (Blayney et al, 1997).

SAMMS was tested in solutions containing the most common and toxic methylmercury compound, CH_3-Hg-OH, that is often found in groundwater. A 10-mg sample of SAMMS #2 was added into 50-mL polypropylene centrifuge tubes containing variable amounts of 0.1 M $NaNO_3$ solution. An aliquot containing a different amount of CH_3-Hg-OH was added to each centrifuge tube containing the SAMMS #2 and also to centrifuge tubes containing no SAMMS to obtain initial organic mercury concentrations. The final volume of the solution in each test was 50 mL. The tubes were then shaken for 4 hours before they were filtered. The filtrates are analyzed for pH and total mercury.

The data in Table 4.4 show that SAMMS removed methylmercury from simulated waste containing 0.1 M $NaNO_3$, decreasing the Hg concentration from 11.9 ppm down to 70 ppb at a ratio of solution volume to SAMMS of 5000. The mercury loading on SAMMS from methylmercury was as high as 566 m/g of SAMMS, which is close to the mercury loading in $Hg(NO_3)_2$ solutions. The isothermo absorption curve is shown in Figure 4.4, which shows that the binding of organic mercury is close to a Langmuri Isotherm behavior at low mercury concentration. The behavior deviates from Langmuri behavior when the mercury concentration is higher. Another distinct difference between the mercury binding in $Hg(NO_3)_2/HgCl_2$ and in $HgCH_3OH$ is the pH differences of the final solutions. The final solution pH went down as SAMMS bound to mercury in $Hg(NO_3)_2/HgCl_2$. The solution pH went up substantially when SAMMS bound organic $HgCH_3OH$ at higher organic mercury concentrations as shown in Table 4.4. This may be explained by the folowing reactions according to Schwarzenbach and Schellenberg (Schwarzenbach and Schellenberg 1965):

$$CH_3-Hg-OH = CH_3Hg^+ + OH^- \quad (9)$$

Table 4.4. SAMMS Binding with Organic Mercury, CH_3-Hg-OH

Hg_{Ini}, ppm	Hg_{Fin}, ppm	pH_{Ini}	pH_{Fin}	Kd	Loading mg/g
11.9	0.07	5.50	5.11	788000	59
38.7	0.29	5.81	5.20	658000	192
98.1	14.8	6.03	6.79	28300	417
148.0	36.8	6.13	7.08	15100	556
187.0	73.8	6.16	7.43	7700	566
253.0	183.1	6.31	7.71	1900	350
362.7	288.0	6.41	7.86	1300	373

At low mercury concentration, the Reaction (9) goes to almost completion and little unassociated CH_3-Hg-OH is left in solution. The initial pH is, therefore, the result of the dissociation of CH_3-Hg-OH in the 0.1 M $NaNO_3$ solution. The CH_3Hg^+ formed in Reaction (9) reacts with SAMMS through

$$CH_3Hg^+ + H-S-SAMMS = CH_3-Hg-S-SAMMS + H^+ \quad (10)$$

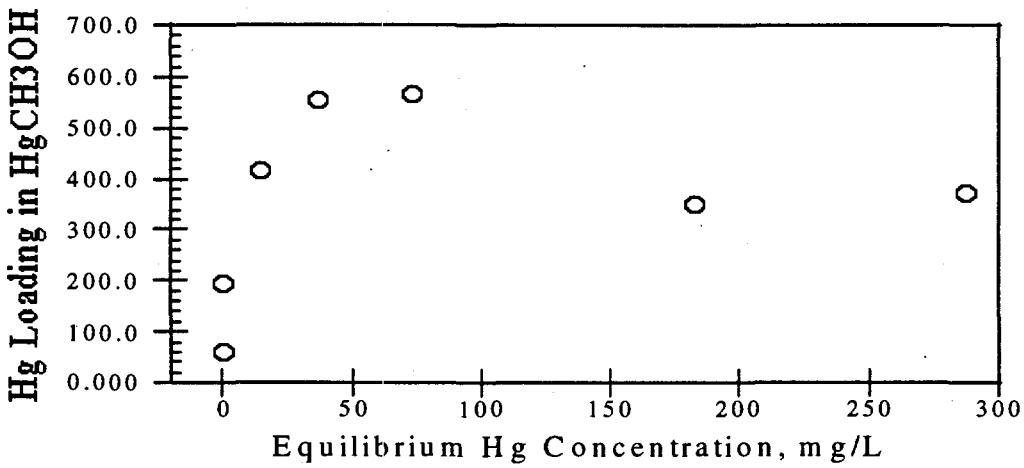

Figure 4.4. SAMMS's Mercury Loading in CH_3HgOH

As a result of Reaction (10), we observed the solution pH decrease when the organic mercury concentrations were low as shown in Table 4.4.

When the concentration of methylmercury is higer, the following reaction becomes significant (Schwarzenbach and Schellenberg 1965):

$$CH_3Hg^+ + CH_3Hg^+ + OH^- = (CH_3Hg)_2OH^+ \qquad (11)$$

As a result of Reaction (11), a high concentration of OH associated in the $(CH_3Hg)_2OH^+$ species. When SAMMS was added to the above reaction mixture, the SAMMS reacted with CH_3Hg^+ through Reaction (10), resulting in the release of hydronium ions. At the same time, the consumption of CH_3Hg^+ had an even larger effect on the equilibrium of Reaction (11) since the equilirium (11) depends on the square term of CH_3Hg^+ concentration. This means the back reaction of equilibrium (11) {i.e., the dissociation of $(CH_3Hg)_2OH^+$} resulted in more hydroxyl ion release than the hydronium ion release from Reaction (10) upon the same change in concentration of CH_3Hg^+. The net result was solution pH increase after adding SAMMS. This also promotes the dissociation of $(CH_3Hg)_2OH^+$ through the reverse of Reaction (11), which increases the solution pH. There may be also other possiblities, such as the following: SAMMS binds to some complexed hydroxyl methylmercury complex, which releases hydroxyl ions instead of hydronium ions to account for the observed solution pH increase upon adding SAMMS. Some of the methylmercury bound SAMMS are being studied using NMR to see what species was bound to SAMMS in the methylmercury solution to help understand the reaction between SAMMS and methylmercury.

Binding to Metallic Mercury: Metallic mercury was reacted with SAMMS #2 under four different conditions: 1) metallic liquid mercury directly contacts with dry SAMMS, 2) metallic mercury vapor contacts with dry SAMMS, 3) metallic liquid mercury directly contacts with SAMMS in aqueous solution,

4) metallic liquid mercury contacts with an aqueous solution that is in contact with the SAMMS powders contained in a membrane bag (i.e., metallic mercury and SAMMS powders were not in direct contact).

In condition 1, where metallic mercury direct contacts with dry SAMMS, a 0.25-g sample of SAMMS #2 was mixed with 0.5 g metallic mercury using a stir bar within a flask for 3 days. The SAMMS powders changed color from white to grey during this period. At the end of 3 days, distilled water was added into the flask. Some of the SAMMS were found to float on top of the solutions and some of them sinked to the bottom of the solution together with some unreacted mercury.

The SAMMS floating on the top of the solution were separated from the unreacted mercury. The floated SAMMS were collected and dried in a hood at room temperature overnight. A total of 0.2076 g of the dried SAMMS powders was treated with 8 mL concentrated HCl, and the solution was analyzed and found to have a mercury concentration of 210 ppm, which is equivalent to 8 mg Hg/g. It is noted that analyzing only the floated SAMMS is not the accurate way to represent the SAMMS binding capacity because the SAMMS powders that absorbed most of the Hg^{2+} in mercury salt solutions are those SAMMS that sank to the bottom of the aqueous solution. The floating SAMMS did not have high mercury loading because of insufficient contact with the wastes. The SAMMS that sank to the bottom of the solution was difficult to separate from the unreacted mercury, so it has not been analyzed.

In condition 2, mercury vapor was generated from a distillation flask that was connected to another flask containing dry SAMMS #2 powders. The flasks were open to each other and were placed in a 50°C water bath to generate low mercury vapor to react with SAMMS for 2 days. The reacted SAMMS was then heated in a mercury-free atmosphere at 60°C to desorb the physically adsorbed mercury. A sample of 0.0821g of the the SAMMS powders was then treated with 8 mL HCl and generated a solution containing 10 ppm mercury, which corresponds to 1 mg mercury/g of SAMMS. The low mercury loading may be due to insufficient mercury vapor generated during the 50°C experiment or due to inability of SAMMS binding to metallic mercury in an oxygen-free environment.

In condition 3, where metallic mercury directly contacted with SAMMS in aqueous solution, a 0.1-g sample of metallic mercury was combined with 0.5 g SAMMS #2 powders in 125-mL bottles; then, a 100-ml solution of 0.1 M $NaNO_3$ was added into the bottles. The metallic mercury inside the bottle was broken down using ultrasonification, and the reaction was allowed to proceed for 3 days at room temperature. At the end of 3 days, the SAMMS floating on the top of the solution and that which sank to the bottom were separated, and mercury was extracted with concentrated HCl. A control test was carried out in the same way without SAMMS. The aqueous solutions from both SAMMS samples and control were analyzed for mercury. The control showed a mercury concentration of 62.5 ppb, which is close to the metallic mercury solubility in water. The mercury concentration was below the detection limit of 10 ppt in the SAMMS sample solution. This result suggests that the presence of SAMMS can effectively remove mercury from water at the presence of metallic mercury. It is expected that the metallic mercury at the bottom of ponds or rivers could be eventually transferred to SAMMS if sufficient time and sufficient amounts of SAMMS are provided and the SAMMS can maintain these water with a mercury contents below drinking water standards at all times. A sample of 0.0836 g of the floating SAMMS was treated with 8.0 mL of concentrated HCl, and the treated solution was analyzed to have 0.688 ppm mercury. The settled SAMMS powders were washed with 0.1 M $NaNO_3$ solution and dried overnight. A sample of 0.4854 g of the SAMMS powders was treated with 8.0 mL of concentrated HCl, and the solution was analyzed to have a mercury concentration of 360 ppm, which corresponds to a mercury loading of about 6 mg/g.

In condition 4, 0.5 g of SAMMS #2 powder was placed in a membrane bag and floated on top of a 0.1 M $NaNO_3$ solution while 0.1 g metallic mercury was placed at the bottom of the 0.1 M $NaNO_3$ solution. The metallic mercury inside the bottle was broken down using ultrasonification, and the reaction was allowed to proceed for 3 days at room temperature. A control experiment was performed using a membrane bag without SAMMS under the same conditions. At the end of 3 days, the mercury concentrations in the control solution and in the SAMMS solution were analyzed. The control solution had a mercury concentration of about 62.5 ppb, which shows that the membrane bag did not sorb mercury. The solutions containing SAMMS bags had a mercury concentration of about 15 and 11 ppb, respectively. This result indicates that the SAMMS powders in the bag can also absorb some of the mercury in solution, but it is not effective because most of the SAMMS powders in the membrane bags were essentially dry at the end of the test.

In all conditions, SAMMS bound to mercury with a mercury loading under the test conditions of 1 to 8 mg/g. SAMMS reduced the solubilized mercury in solutions containing metallic mercury below 10 ppt.

4.5 pH Effects

It is seen from the above discussion that the binding reaction of SAMMS with mercury may involve release of hydronium ion, which affects solution acidity. It is necessary to study how solution pH affects the mercury separation of SAMMS, especially waste solutions that exist in a broader range of pHs.

A 10-mg sample of SAMMS #2 was added by pipetting 2 mL SAMMS working slurry into 50-mL polypropylene centrifuge tubes containing an aliquot of 48 mL 0.1 M $NaNO_3$ solutions that were previously spiked with 0.1 M $Hg(NO_3)_2$ solution to provide an initial total mercury concentration of 0.0001 M and were adjusted to a range of pH from 3 to 10 using 0.1 M HNO_3 or NaOH. The slurries were then shaken for 4 hours before they were filtered with syringe filters. Each test at each pH was conducted in duplicate. Control tests at each pH without SAMMS were also conducted. The solutions were analyzed for pH and total mercury before and after equilibrium with SAMMS.

The results on pH effects are summarized in Table 4.5 and Figure 4.5. It clearly shows a pH effect on the mercury binding by SAMMS: SAMMS achieves the highest Kds in the pH range of 5.7 to 6.7. The Kd value decreased six times when the solution pH was increased from pH 6.7 to 9.2. The Kd decreased 48 times when the solution pH was decreased from 6.7 to 2. This may be because the thiol group on SAMMS is a weak acid. At pH 6.7, it is almost fully dissociated as an anonic species that is most favorable to react with the positively charged mercury species as:

$$Hg(OH)^{+} + {}^{-}S\text{-}SAMMS = HO\text{-}Hg\text{-}S\text{-}SAMMS \qquad (12)$$

At lower pH, the thiol group on SAMMS becomes protonated as a neutral species, and Reaction (12) becomes more difficult. At higher pH, the mercury species become a neutral species such as $Hg(OH)_2$ or negatively charged species such as $Hg(OH)_3^-$, and the above reaction is also less effective.

Table 4.5. pH Effects on SAMMS' Mercury Binding

pH Ini	pH Fin	C_{ini} ppb	C_{fin} ppb	Kd
2.0	2.0	19900.0	100.3	9.9E+05
3.0	2.9	19850.0	68.5	1.4E+06
4.0	4.0	19800.0	6.8	1.5E+07
4.5	4.6	19750.0	5.2	1.9E+07
5.0	5.1	19725.0	5.8	1.7E+07
6.0	5.7	19700.0	2.5	3.9E+07
7.0	6.2	19600.0	2.5	3.9E+07
8.0	6.7	19450.0	2.0	4.8E+07
9.5	7.0	19200.0	7.6	1.3E+07
10.0	9.2	18900.0	12.5	7.6E+06

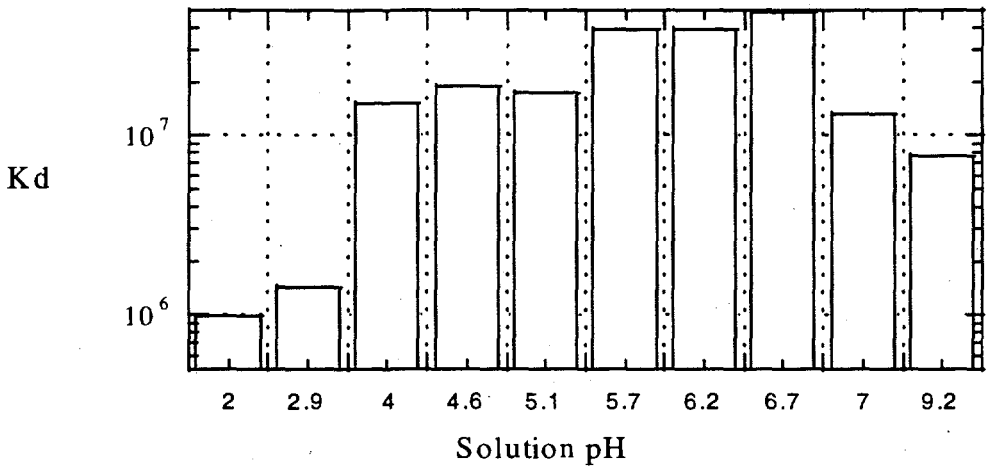

Figure 4.5. pH Effects on SAMMS' Hg Binding

4.6 Ionic Strength Effects

In general, the activities of the thiol groups on the SAMMS and the mercury ions in solutions are affected by solution ionic strength, and the SAMMS's efficiency of binding mercury may also be affected by waste solutions with very different ionic strength, such as low ionic strength groundwater to concentrated salty tank wastes. A 10-mg sample of SAMMS is added by pipetting 2 mL SAMMS slurry into 50-mL polypropylene centrifuge tubes containing an aliquot of 47.95 mL of $NaNO_3$ solution (at pH 5.0) with the concentration ranging from 0 to 4.0 M. The slurries are spiked with 0.05 mL of 0.1 M

$Hg(NO_3)_2$ stock solution to provide an initial concentration of 20.8 mg/L. The slurries are then shaken overnight before ~~it is~~ they are filtered with a syringe filter. The experiments were conducted in triplicate. The filtrates are analyzed for total mercury before/after equilibration with SAMMS.

The results are listed in Table 4.6 and Figure 4.6. In comparison with pH effects, the ionic strength effects on SAMMS's mercury-binding efficiency were much less pronounced. It showed a slightly decreasing Kd as the ionic strength of the solution was increased from deionized water to 1 M $NaNO_3$ solution. However the Kd differences are less than a factor of 3. Furthermore, there were no obvious ionic strength effects on Kd when the $NaNO_3$ concentration increased from 2 to 4 M.

Table 4.6. Ionic Strength Effects on Hg Binding Kd

$NaNO_3$ M	Cini ppb	Cfin ppb	pH Final	Kd
0.00	20800	1.9	3.4	5.47E+07
0.05	20800	1.9	3.5	5.53E+07
0.10	20800	2.9	3.5	3.54E+07
0.30	20800	3.2	3.6	3.25E+07
0.60	20800	4.3	3.6	2.44E+07
1.00	20800	5.5	3.5	1.88E+07
2.00	20800	1.9	3.4	5.47E+07
3.00	20800	2.0	3.3	5.31E+07
4.00	20800	1.9	3.2	5.59E+07

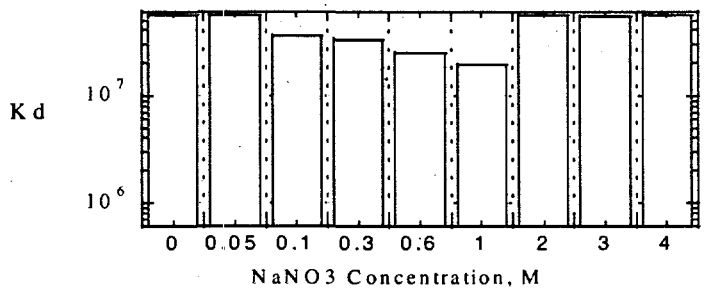

Figure 4.6. Ionic Strength Effects on SAMMS' Hg Binding

4.7 Cation Effects

Waste solutions always contain many other cations besides mercury. How the other cations compete with mercury to bind to mercury should depend on the characteristics of each cation. The thiol group HS- on SAMMS is a soft base, and it preferentially binds to soft acids such as Hg^{2+} and $Hg(OH)^+$. Of course, other soft bases, such as Ag^+, Cu^+, and Cu^{2+}, may also compete with mercury to bind the thiol groups that will affect the selectivity of SAMMS for mercury as well as the mercury loadings on SAMMS.

In this experiment, SAMMS was added to a 0.1 M $NaNO_3$ solution containing an equal molar concentration of mercury and a prospective cation such as Ca(II), Fe(II), Pb(II), Cu(II), Cd(II), Ni(I), and Zn(II) to see how each cation affects SAMMS's behavior in mercury binding. Three additional solutions containing three (Cd, Ni, and Zn), four (Cu, Pb, Ca, Fe), and seven (Ca, Cd, Cu, Fe, Ni, Pb, and Zn) cations with the molar concentration ratio to mercury of 3, 4, and 7, respectively, were also prepared. Half of each cation solution was adjusted to pH 4, and the other half were adjusted to pH 7. A 10-mg quantity of SAMMS was added to each 48.5 mL of the cation solution as 1.5 mL slurry, and the solution was then shaken for 4 hours before filtration and measurement of final pH. The filtrate was analyzed for mercury. The results are shown in Table 4.7 and Figure 4.7.

In pH 7 solutions, the effectiveness of cations in reducing mercury binding of SAMMS follows the order (Figure 4.7b):

$$Cd(II) > Pb(II) > Fe(II) > Cu(II) > Ni(I) >/= Zn(II) > Ca(II)$$

This order is similar to its sofness of the cations, i.e., Cd(II) is the softest cation and it reduced the mercury-binding Kd by 400 times from 1.14×10^8 down to 2.73×10^5. The hard ion Ca(II) exhibited no interference with mercury binding. It is also interesting to see (Figure 4.7b) that more cations in the solution diluted the interferring ability of cations (Table 4.7): the Kd in the single component Cd solution was 2.73×10^5 by comparing the results; Kd increased to 4.65×10^6 in the 3-cation solution where the Cd concentration was the same as the single component Cd solution, and the Kd reached 4.15×10^7 in the 7-cation solution. These effects can also be see by comparing the following Kds at pH 7:

Kd	Pb, M	Other Cation, M (not considering Na)	Solution ID
1.75×10^6	1×10^{-4}	0.0	Pb
1.10×10^7	1×10^{-4}	3×10^{-4}	4Cat
4.15×10^7	1×10^{-4}	6×10^{-4}	7Cat

The cation effects on decreasing the mercury binding of SAMMS in pH 4 solution (Figure 4.7a) follows the order of

$$Fe(II) > Cd(II) > Pb(II) > Ni(I) > Zn(II) > Ca(II) > Cu(II).$$

This order is slightly different from the order at pH 7. In particular, the Cu(II) showed less interference than even Ca. It is understandable that the effectiveness order changes with solution pH since the pH change induces the softness change on both the thiol groups (from SAMMS-S^- to SAMMS-SH) and on cations (different extent of hydrolysis on cations). The observation that at pH 7, the single cation solution is more effective to interfere with SAMMS mercury binding than multiple cations at the same cation concentrations is also true at pH 4.

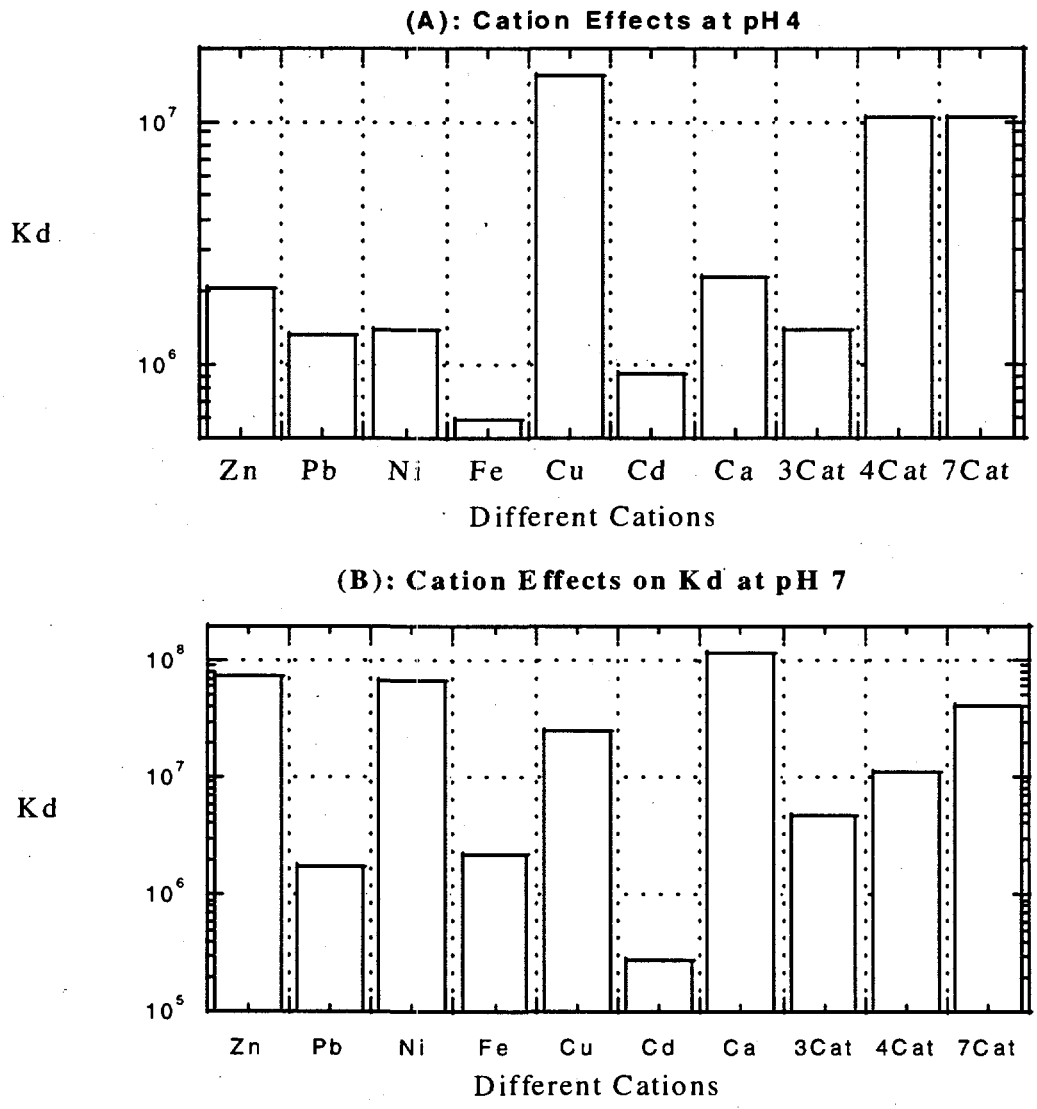

Figure 4.7. Cation Effects on SAMM's Mercury Binding (A) at pH 4 and (B) at pH 7

In summary, the overal interference from common cations such as Na (seen from the ionic strength effect experiment discussed in Section 4.6), Ca, Zn, and Ni on mercury binding of SAMMS is minimal. The Kd for mercury binding is still as high as 2.73×10^5, even at the presence of the most interfering cation of Cd(II). The interference from cations is also minimal when more than seven cations exist since the Kd was observed to be at least 1×10^7 in these solutions.

Table 4.7. Cation Effects on SAMMS's Mercury Binding

	At pH 4					At pH 7				
	Hg(in) ppb	Hg(fi) ppb	pH(in)	pH(fi)	Kd	Hg(in) ppb	Hg(fi) ppb	pH(in)	pH(fi)	Kd
Zn	18700	45.3	4.02	3.93	2.06E+06	19100	1.3	7.08	5.14	7.21E+07
Pb	18400	68.3	3.94	3.74	1.34E+06	18800	53.7	6.94	4.20	1.75E+06
Ni	18700	66.5	4.02	3.87	1.40E+06	19000	1.4	7.10	6.02	6.79E+07
Fe	17900	151.5	4.06	3.98	5.86E+05	15700	36.0	7.02	5.75	2.18E+06
Cu	18600	6.1	3.80	3.58	1.54E+07	19100	3.9	7.08	4.64	2.48E+07
Cd	18200	99.5	4.00	3.69	9.10E+05	18800	338.3	7.13	4.27	2.73E+05
Ca	18600	40.8	4.05	3.77	2.28E+06	18600	0.8	6.88	5.77	1.14E+08
3Cat	18100	65.6	3.89	3.71	1.38E+06	18100	19.5	6.83	4.18	4.65E+06
4Cat	18200	8.8	4.05	3.68	1.03E+07	17700	8.1	6.97	5.10	1.10E+07
7Cat	18300	8.9	4.01	3.65	1.03E+07	18300	2.2	6.99	4.87	4.15E+07

4.8 Anion Effects

Many anions in ground waters and in waste streams may form complexes with mercury in solution, which may affect the ability of SAMMS to remove mercury from the groundwater and waste streams.

In this experiment, $Hg(NO_3)_2$ solutions containing Cl^-, CN^-, CO_3^{2-}, SO_4^{2-}, and PO_4^{3-} were prepared. The anion concentrations were 0.5, 1, 5, and 10 times of mercury concentration on a molar basis. $NaNO_3$ was used to maintain a constant ionic strength of 0.1 M. A 10-mg quantity of SAMMS was added to each of 50-mL anion solution and was shaken for 4 hours before filtration with syringe filters. The filtrate was analyzed for mercury. Each anion solution was tested at both pH 4.0 and 7.0 in duplicate.

The results are shown in Table 4.8 and Figure 4.8. At both pH 4 and 7, CN^- was the least in reducing the SAMMS mercury binding Kd, and the other anions reduced the Kd by about 5 times. Anion concentration changing by 100 times (from 0.1 to 10×10^{-4} M) did not show substantial effects on the anion effects. At pH 7.0, the decreasing order of its ability to influence the mercury-binding Kd of SAMMS is

$$Cl^- > SO_4^{2-} > CO_3^{2-} > PO_4^{3-} > CN^-$$

This order did not change with the anion concentration range tested. At pH 4, the effects are similar to that at pH 7, and it is difficult to determine the pattern in the order among Cl^-, CO_3^{2-}, SO_4^{2-}, and PO_4^{3-}, especially when the anion concentration changes. Also, the influence of anions among Cl^-, CO_3^{2-}, SO_4^{2-}, and PO_4^{3-} is of a similar magnitude.

4.9 Demonstration on Simulated Aqueous and Oil Wastes and Actual SRS (Savannah River Site) Tritiated Pump Oil Wastes

Preliminary trials of the mercury-binding capabilities of SAMMS #1 were conducted in simulated wastewater of SRS radioactive waste-holding Tank L (compositions were shown in Table 4.9 as before SAMMS absorbtion) and simulated nonradioactive vacuum pump oil waste of the SRS Tritium Facilities.

The analyzed compositions of wastewaters at pH 3, 7, and 9 and the oil waste are shown in Table 4.9. These waste solutions were mixed with SAMMS #1 powders at volume ratios of waste-to-SAMMS ranging from 20 to 100 (Table 4.10) at room temperature for 2 hours. The remaining RCRA metals in solutions were analyzed using cold vapor atomic absorption for mercury and inductively coupled plasma-atomic emission spectroscopy (ICP-AES) for other metals, as shown in Table 4.9. SAMMS #1 reduced the mercury concentration from 6.35 ppm to 0.7 ppb (below the drinking water limit of 2 ppb) by just one treatment of wastewater 38 times its volume. The distribution coefficient is as large as 340,000 at a pH range from 3 to 9 and with the presence of large concentrations of other cations (e.g., 2220 ppm Na and 7 ppm of Ba). The RCRA metals, Pb, Ag, and Cr, were also reduced to below RCRA levels at pH 7 and 9. SAMMS reduced the mercury level from 12.1 ppm to 0.066 ppm (the hazardous waste limit is 0.2 ppm) by treating 20 times the waste oil volume once.

Actual tritiated vacuum pump oil wastes generated in the SRS Tritium Facilities were tested at Oak Ridge National Laboratory using the SAMMS powders. Samples (3 mL) of SRS tritiated pump oils were mixed with 0.01 to 0.3 g of SAMMS, and the mixtures were equilibrated for 48 hours before they were filtered and analyzed for mercury. All the tests were performed in duplicate. Another two sorbents, sulfur and sulfur-impregnated activated carbon (SIAC), were tested under similar conditions for comparison. A control test without sorbent was also tested with two different SRS pump oils. Laboratory batch tests successfully removed 91%of the mercury from samples of actual tritiated waste oils generated in the SRS Tritium Facilities. Only 2 to 29% of mercury was removed using sulfur-impregnated carbon and sulfur under the same test conditions.

The results in Table 4.11 and Figure 4.9 show that SAMMS was able to remove up to 91% of the mercury in the tritiated pump oils through the single treatment. The removing efficiencies for sulfur and sulfur-impregnated activated carbon were 28 and 9% respectively. The Kd for SAMMS in the actual tritiated pump oil was up to 3.47×10^5, and the observed mercury loading was up to 13.59 mg/g.

4.10 Toxicity Characteristic Leach Procedure (TCLP) on Mercury-SAMMS

The RCRA-laden SAMMS #1 may be disposed of directly as solid wastes because they passed TCLP tests by showing up to 1000 times lower release of RCRA metals (Table 4.12).

4.11 Chemical Stability and Aqueous Durability of Mercury-SAMMS

The chemical stability of mercury-SAMMS was evaluated by 1) evaluating the mercury loss and binding change using NMR after heating the mercury-SAMMS #1 powders in the air for 75 and 125°C for 24 hours and 150°C in air for 50 hours, and 2) by measuring the mercury concentration in solution after mercury-SAMMS #2 was heated in water at 70°C for 24 hours.

Table 4.8. Anion Effects

ID	pH, ini	pH, fin	Hg(in), ppb	Hg(in) ppb	Kd
0.5CL4	4.00	3.85	19800	30.1	3.29E+06
0.5CN4	4.00	3.97	19800	7.7	1.29E+07
0.5CO4	4.00	4.00	19800	40.8	2.42E+06
0.5SO4	4.00	4.09	19800	41.6	2.37E+06
0.5PO4	4.00	4.04	19800	26.5	3.73E+06
1CL4	4.00	3.72	19800	28.4	3.48E+06
1CN4	4.00	3.99	19800	6.1	1.64E+07
1CO4	4.00	4.01	19800	34.9	2.83E+06
1SO4	4.00	4.02	19800	41.5	2.38E+06
1PO4	4.00	4.03	19800	29.2	3.39E+06
5CL4	4.00	3.61	19800	29.8	3.32E+06
5CN4	4.00	4.04	19800	2.7	3.74E+07
5CO4	4.00	4.02	19800	27.0	3.67E+06
5SO4	4.00	4.03	19800	30.9	3.20E+06
5PO4	4.00	4.02	19800	26.4	3.75E+06
10CL4	4.00	3.63	19800	36.4	2.71E+06
10CN4	4.00	4.05	19800	3.1	3.25E+07
10CO4	4.00	4.00	19800	35.2	2.81E+06
10SO4	4.00	4.02	19800	34.6	2.86E+06
10PO4	4.00	4.04	19800	27.4	3.61E+06
0.5CL7	7.00	5.28	19600	33.0	2.97E+06
0.5CN7	7.00	5.64	19600	3.0	3.27E+07
0.5CO7	7.00	5.60	19600	18.1	5.42E+06
0.5SO7	7.00	5.44	19600	25.7	3.82E+06
0.5PO7	7.00	6.36	19600	12.0	8.16E+06
1CL7	7.00	5.30	19600	29.9	3.28E+06
1CN7	7.00	5.27	19600	3.1	3.21E+07
1CO7	7.00	6.00	19600	21.1	4.65E+06
1SO7	7.00	6.20	19600	24.1	4.07E+06
1PO7	7.00	6.83	19600	11.4	8.63E+06
5CL7	7.00	4.60	19600	30.1	3.26E+06
5CN7	7.00	5.69	19600	1.7	5.94E+07
5CO7	7.00	7.07	19600	16.1	6.08E+06
5SO7	7.00	5.92	19600	17.9	5.47E+06
5PO7	7.00	6.93	19600	12.9	7.62E+06
10CL7	7.00	4.40	19600	27.0	3.62E+06
10CN7	7.00	6.01	19600	3.1	3.16E+07
10CO7	7.00	7.28	19600	17.2	5.71E+06
10SO7	7.00	5.89	19600	16.3	6.01E+06

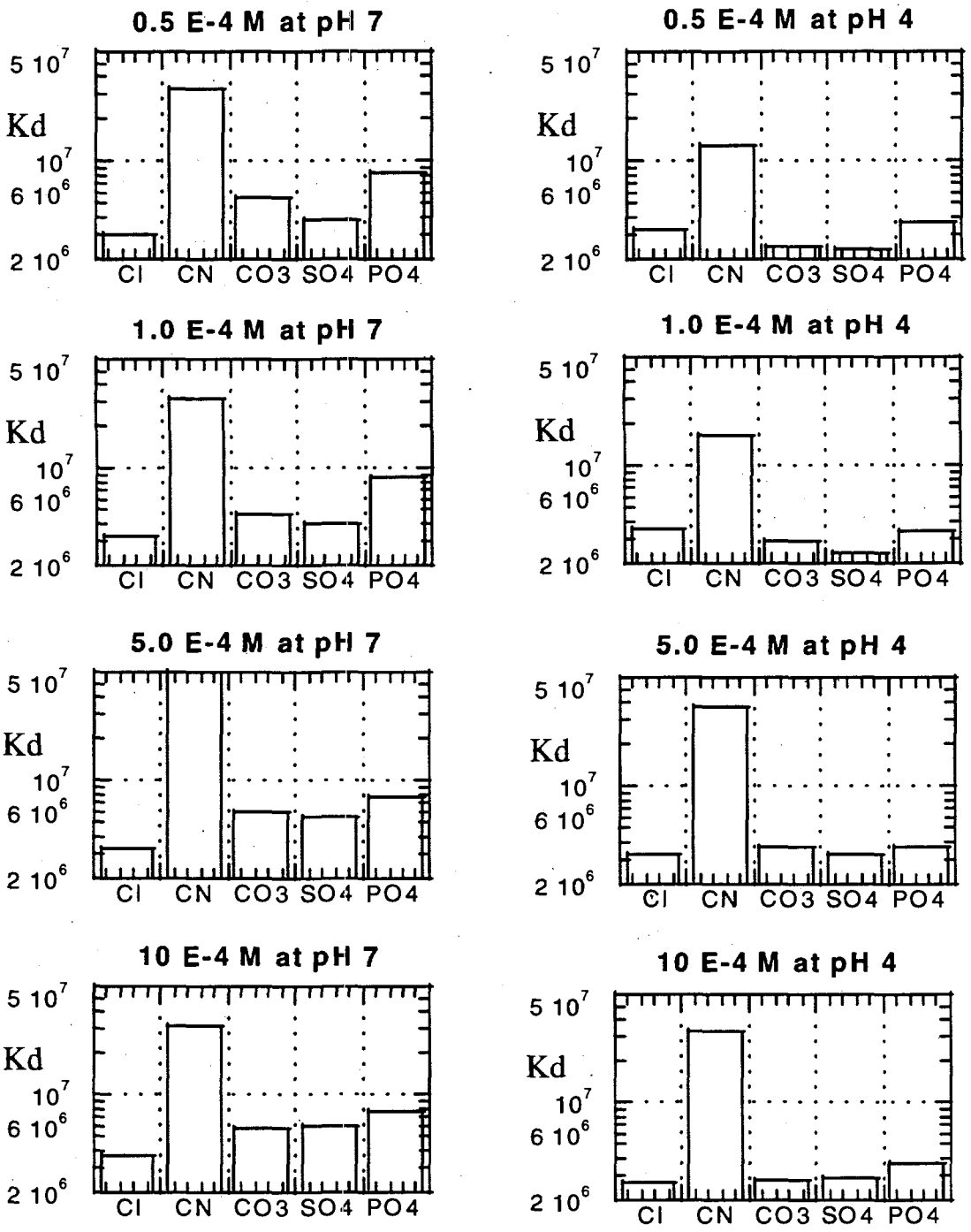

Figure 4.8. Anion Effects on SAMMS's Mercury Binding. The anions have concentrations of 0.5×10^{-4}, 1×10^{-4}, 5×10^{-4}, and 10×10^{-4} at pH 4 and pH 7

Table 4.9. Analyzed RCRA Metal Concentrations (ppm) in Waste Solutions Before and After SAMMS #1 Treatment

	Hg	Ag	Cr	Pb	Ba	Zn	Na
Before:							
WW at pH 3	6.20	1.80	1.79	7.22	7.18	3.96	2220
WW at pH 7	6.00	0.45	1.13	5.25	7.12	2.75	2212
WW at pH 9	6.35	1.04	0.58	2.90	7.15	1.32	2222
Oil-1	12.10						
After:							
SAM-1-3	0.0108	<.005	1.45	1.66	7.60	3.93	2236
SAM-1-7	0.0064	<.005	0.70	0	7.35	2.23	2202
SAM-1-9	0.0056	<.005	0.71	0	7.40	1.41	2218
SAM-2-3	0.0008	<.005	1.67	2.26	8.64	5.06	2185
SAM-2-7	0.0008	<.005	0.07	0	8.21	1.54	2114
SAM-2-9	0.0007	<.005	0	0	8.82	1.19	2201
SAM-1-Oil	0.635						
SAM-2-Oil	0.066						

Previous characterization of these mercury-laden materials indicates that the mercury is directly bound to the monolayer via an Hg-S bond and that neighboring mercury atoms are linked by an oxo bridge (Hg-O-Hg) (Feng et al 1997b). The chemical shifts reported above for both the primary and secondary products are most consistant with oxygen-based functionality (Levy et al. 1980).

Subjecting the mercury-laden SAMMS to heat results in a slow, steady chemical change taking place at the monolayer interface. This chemistry is easily monitored by solid-state ^{13}C NMR (see Figure 4.10). The carbon resonance appearing at 13 ppm in all of these spectra is readily assigned to the methylene bound to the silicon atom and can be used a type of internal standard since it remains unchanged throughout this chemistry.

The two peaks at 28 and 37 ppm (assigned to the internal and thiol-bearing methylenes, respectively) are seen to slowly disappear during this thermolysis, suggesting that the terminal mercury thioalkoxide is undergoing some sort of chemical change. As the original signals decay, other features are seen to grow into the spectrum. The first, and most notable, of these is the peak at 55 ppm, first seen in the 75°C spectrum. Concomittantly, a partially obscured peak appears at approximately 20 ppm. As the

Table 4.10. Testing Parameters of the Simulated Wastes Using SAMMS #1

	Types of Wastes	V_{waste}/V_{SAMMS}	K_d of Hg	Remaining Hg in Waste (ppb)
SAM-1-3	Waterwater at pH 3	97	55670	10.8
SAM-1-7	Waterwater at pH 7	97	90974	6.4
SAM-1-9	Waterwater at pH 9	97	110056	5.6
SAM-2-3	Waterwater at pH 3	38	290588	0.8
SAM-2-7	Waterwater at pH 7	38	281213	0.8
SAM-2-9	Waterwater at pH 9	38	340141	0.7
SAM-1-Oil	Waste pump oil	100	1806	635
SAM-2-Oil	Waste pump oil	20	3647	66

Table 4.11. Mercury Removal From Actual SRS Tritiated Pump Oils

Sorbent	Sobent g	Initial mg/Kg	Final mg/Kg	Kd	Loading mg/g	Dec. %
Control-1	0.00	52.1	43.5			
SAMMS	0.20	52.1	6.0	1.16E+05	0.69	89
Sulfur	0.20	52.1	37.3	5.95E+03	0.22	28
SIAC	0.20	52.1	47.3	1.52E+03	0.07	9
Control-2	0.00	84.5	61.4			
SAMMS	0.01	84.5	39.2	3.47E+05	13.59	54
SAMMS	0.05	84.5	34.8	8.57E+04	2.98	59
SAMMS	0.10	84.5	33.0	4.68E+04	1.55	61
SAMMS	0.30	84.5	7.6	1.01E+05	0.77	91

temperature is raised to 125°C, both of these features are enhanced and are accompanied by a peak at about 25 ppm, as well as multiple overlapping poorly defined resonances between 62 and 75 ppm. Raising the temperature to 150°C results in further depletion of the original signals at 37 and 28 ppm, as well as the primary product signals at 55 and 20 ppm, while enhancing the signals at 25 ppm and 62-75 ppm, consistent with these arising from secondary product formation.

The resonances observed for the primary product are consistent with the formation of a mercuric alkoxide; the terminal oxygen-bearing methylene is at 55 ppm and in the internal methylene is found at 20 ppm (the greater charge separation of the mercuric alkoxide results in more effective shielding of the internal methylene relative to the thioalkoxide).

Table 4.12. TCLP Leachate Concentrations (ppm)

	Hg	Ag	Cr	Pb	Ba	Ni	Zn
SAM-1-Oil	0.0043	0	0	0	0.37	0.10	0.57
SAM-2-Oil	0.0018	0	0	0	0.18	0	0.29
SAM-1(pH 3,7,9)	0.0009	0	0.24	0	0.70	0.20	1.05
SAM-2-3	0.0006	0	0.07	0	0.58	0.06	0.33
SAM-2-7	0.0006	0	0	0	0.55	0	0.31
SAM-2-9	0.0002	0	0	0	0.44	0	0.3
EPA TCLP Limits	0.2	5.0	5.0	5.0	100		
Land Disposal Limits		0.072	5.2	0.51			0.32
Drinking water limit	0.002						

Note: "0" concentration means the concentration below the detection limits of ICP-AES

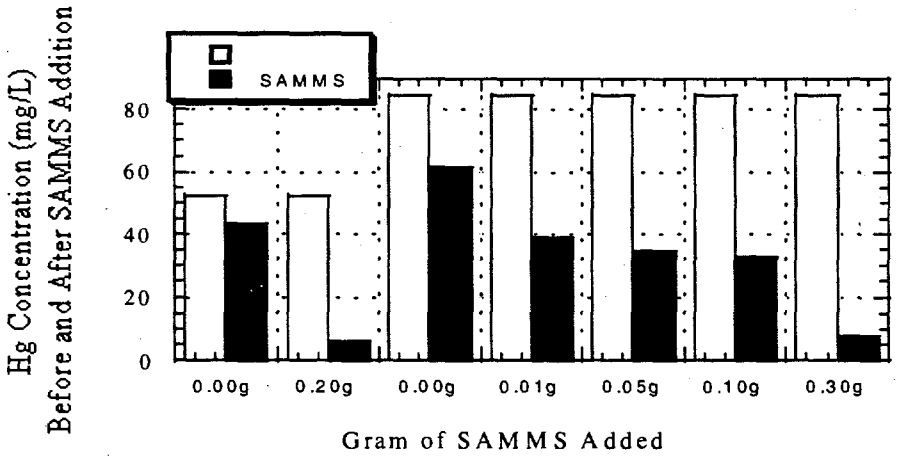

Figure 4.9. Mercury Removal from Actual SRS Tritiated Pump Oil Wastes with SAMMS

The resonances observed for the secondary products are consistant with the hydrolysis, and possible condensation, of the sulfide-bridged mercuric alkoxide intermediate. The poorly resolved signal found at approximately 65 ppm is quite characteristic of the formation of a primary alcohol (structure **3** of Figure 4.11) via hydrolysis of the intermediate mercuric alkoxide (structure **2**) (Levy et al. 1980). This peak is seen to grow in at the same time as the signal at 25 ppm, which is readily assigned to the internal carbon of the primary alcohol. At the same time, a poorly defined peak at about 73 ppm is seen, which is most consistant with formation of a terminal ether (structure **4**) via condensation chemistry (Levy et al. 1980). The internal methylene resonance of the propyl ether is presumably buried beneath the several overlapping signals and is not visible in these spectra.

Mechanistically, this can be viewed as a Lewis acid-induced cleavage of the C-S bond, followed by rearrangement to afford a sulfur-bridged mercuric alkoxide (**2**). This rearrangement replaces a relatively weak C-S sigma bond with a much stronger C-O sigma bond and the bridging oxide with a much more favorable sulfide bridge. These two factors clearly provide the thermodynamic driving force for this rearrangement.

It is worthwhile to note that even after several days at elevated temperatures, a significant portion of mercuric thioalkoxide still remains on the surface. In this mechanism, only half of the thioalkoxide is consumed, consistant with this observation.

The secondary reaction processes then slowly deplete the population of this intermediate product. Once formed, the bridging mercuric alkoxide can suffer one of two fates: simple hydrolysis (to afford the observed primary alcohol), or an interesting internal condensation reaction to afford the corresponding ether. Once again, the first step in this process is a Lewis acid-induced cleavage of a C-S sigma bond. However, the following step involves migration of an alkoxide instead of a metal-oxo bridge. Again, the driving force for this process is the formation of a strong C-O bond at the expense of a weaker C-S bond, as well as the formation of mercuric sulfide.

In summary, the mercury bound to SAMMS is chemically stable. Upon heating to a higher temperature in air, molecular structuares of mercury-SAMMS are rearranged to form a more stable mercury configuration. However, the total amount of mercury bound to SAMMS did not change as a result of heating up to 150°C. From the point of view of mercury-SAMMS as a permanent waste form, this NMR study may provide a molecular understanding of its chemical durability. A total mercury analysis may also be needed to confirm the proposed structural rearrangement, and a TCLP test on the heated mercury-SAMMS may also provide important information about its durability.

4.11.1 Hydrothermal Stability Testing

Samples of mercury-SAMMS #2 with mercury loading of 503 mg/g were used for this evaluation. These samples were washed with a few mLs of deionized water before drying. A 0.05-g quantity of the mercury-SAMMS #2 was added to 50.0 mL deionized water in a Teflon vessel, mixed well, and kept at 70°C for 24 hours. The test was duplicated. At the end of the 24 hours, the solutions were filtered, and the filtrate was analyzed. The duplicate tests had mercury concentrations of 12.7 and 13.0 mg/L, respectively.

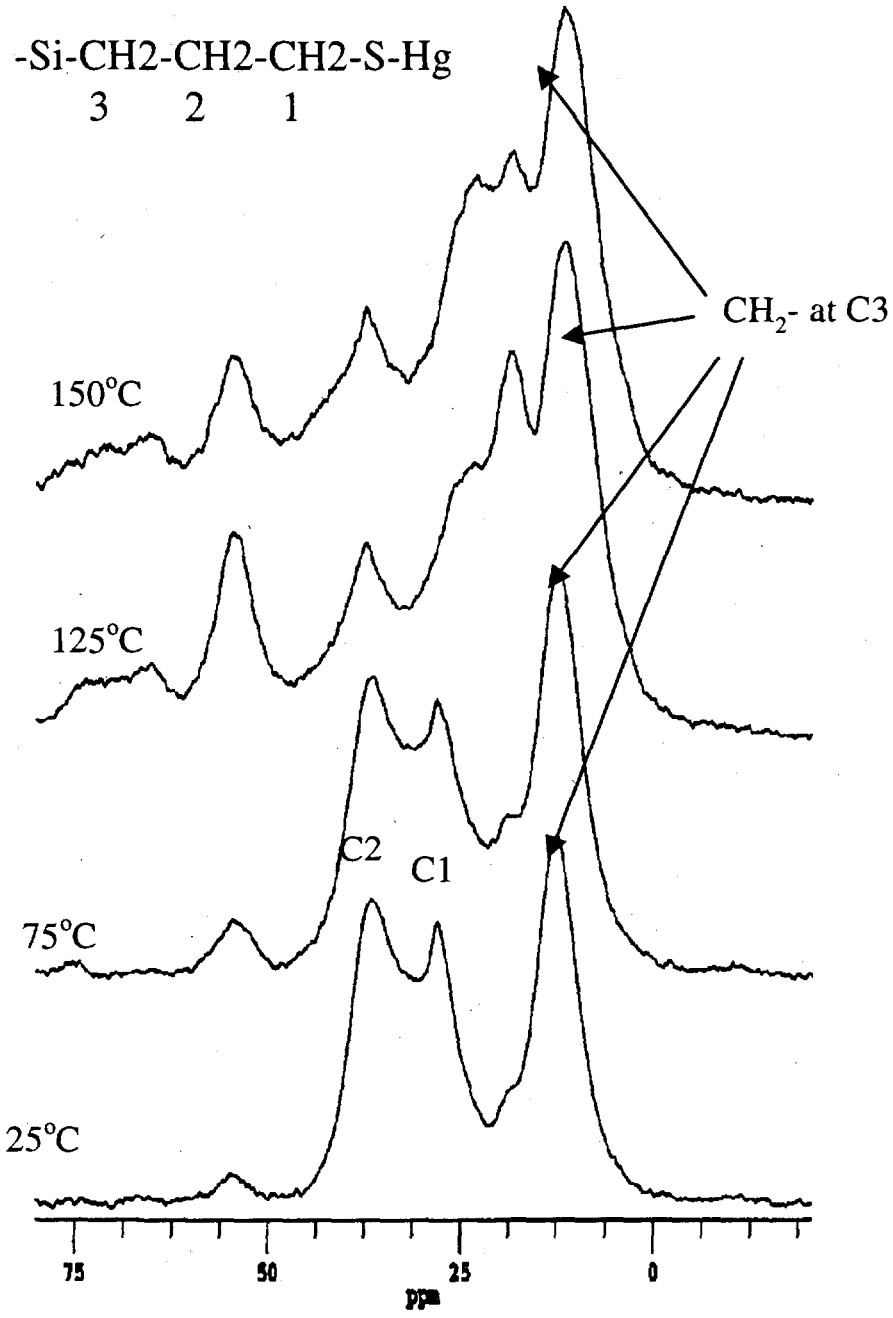

Figure 4.10. NMR Spectra of Mercury-SAMMS at Room Temperature, after Heating at 75 and 125°C in air for 24 Hours, and after Heating at 150°C in Air for 50 Hours

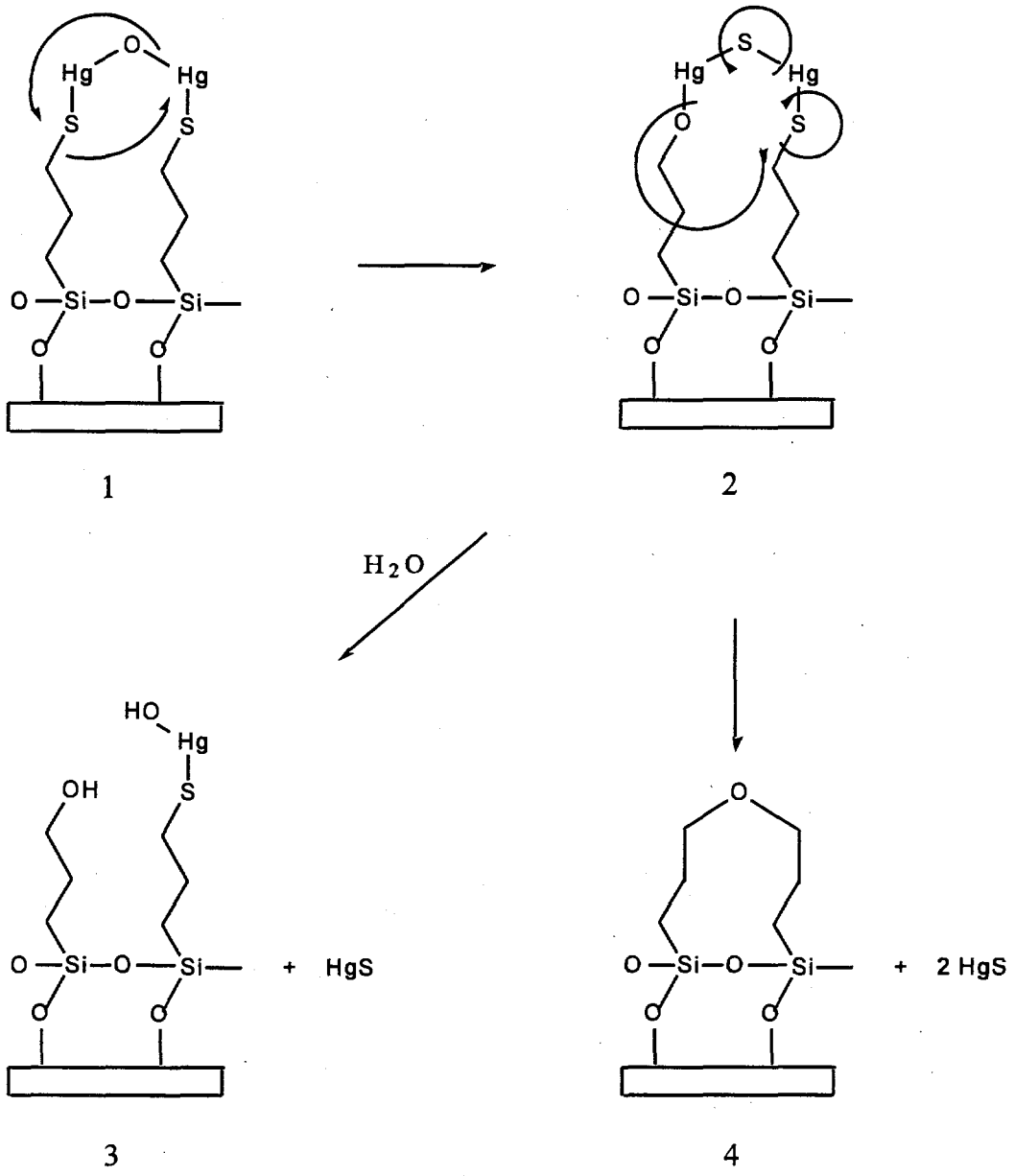

Figure 4.11. Thermo Rearrangement of Mercury-SAMMS During Heating

Because the mercury-SAMMS #2 powders used for the tests were not washed thoroughly, some mercury released simply may have been due to the surface-adsorbed mercury; a blank test was carried out. In the duplicate blank tests, the same mercury-SAMMS #2 powders were treated in the same way as for the 70°C tests, except that the mixture solutions were kept at room temperature. At the end of the 24 hours, the solutions were filtered and analyzed to find a mercury concentration of 10.5 and 10.6 mg/L, respectively, which is very similar to the 70°C tests. This result may suggest that most of the mercury released was due to the adsorbed mercury instead of the high temperature (70°C in this instance)

hydrolysis of the mercury-SAMMS. Previously, mercury-SAMMS #1 was tested in a pH 4.7 sodium acetate solution of the TCLP test; only 0.02 ppb mercury was found in the solution after 24 hours of testing at room temperature because these mercury-SAMMS #1 powders were washed thoroughly with several liters of deionized water.

The mercury release results of the mercury-SAMMS #2 are very similar at room temperature and at 70°C, suggesting high stability of the mercury-SAMMS at 70°C. A complete release of mercury from the 0.05 mercury-SAMMS in 50.mL water would result in a mercury concentration of 335 mg/L. By subtracting the mercury released through the blank, the total release of mercury from the 70°C test is 2.2 and 2.4 mg/g, respectively. In comparison to a total loading of 503 mg/g, this corresponds to 0.4% at 24 hours heating at 70°C.

4.12 A Permanent Waste Form and Regeneration

The mercury-loaded SAMMS not only passed TCLP tests, as shown in Section 4.10, but also had good chemical durability. The mercury-SAMMS therefore is expected to have good long-term durability as a permanent waste form because 1) the covalent binding between mercury and SAMMS has good resistance in ion exchange, oxidation, and hydrolysis over a wide pH range, and 2) the uniform and small pore size (2 to 40 nm) of the mesoporous silica prevents bacteria (at least 2000 nm in size) from solubilizing the bound mercury (microbes are mainly responsible for solubilizing the mercury compounds in the environment into the deadly methylmercury, such as CH_3-Hg-OH). The SAMMS technology is superior to many existing technologies because of the direct generation of a stable waste form that does not require secondary treatment. More systematic study is needed to fully demonstrate SAMMS's advantages as a permanent waste form.

There is still interest, however, in its capability to be regenerated for some special application such as mercury recycle. The following regeneration experiments were carried out.

The Regeneration of Mercury-SAMMS (all the tests are duplicated).

1. First loading with mercury: 0.5163 g of SAMMS #2 was added to 1 L of 0.1 M $NaNO_3$ solution containing 330 mg Hg/L, and the mixture was agitated for 4 hours at room temperature. The mixture was filtered, and the mercury-SAMMS powders were washed with high purity water and air-dried overnight. By analyzing the mercury concentrations of the blank solution (where no SAMMS was used, but same agitation and filtering were applied) and the final solution (filtrate from the SAMMS added solution), a mercury loading of 445 mg mercury/g of SAMMS #2 was obtained.

2. First regeneration: 0.2 g of mercury-SAMMS (dried overnight) was added to 10.0 mL high purity concentrated HCl (37 wt%) solution for 4 hours. The solid SAMMS was then separated by filtration. By analyzing the mercury concentration in the filtrate and comparing it with the available mercury on the SAMMS, it was found that 100% of the mercury was released from the SAMMS. The analyzed Si concentration in the concentrated HCl was only 2.90 ppm, suggesting the silica matrix of the mercury-SAMMS was not damaged by the concentrated acid.

3. Regeneration with 2 N HCl:0.2 g of mercury-SAMMS (dried overnight) was added to 20.0 mL high purity 2 N HCl solution for 4 hours. The solid SAMMS was then separated by filtration. By

analyzing the mercury concentration in the filtrate and comparing it with the available mercury on the SAMMS, it was found that less than 14% of the bound mercury was released from the SAMMS.

4. Second loading with mercury: The regenerated SAMMS (through concentrated HCl) was washed with high purity water thoroughly and air-dried overnight. A sample of 0.075 g regenerated SAMMS was added to 150 mL of 0.1 M $NaNO_3$ solution containing 330 mg Hg/L, and the mixture was agitated for 4 hours at room temperature. The mixture was filtered, and the mercury-SAMMS powders were washed with high-purity water and air-dried overnight. By analyzing the mercury concentrations of the blank solution and the final solution, a mercury loading of 210 mg Hg/g of SAMMS was obtained. This was about 50% of the original loading. This may due to partial oxidation of the functional group on the SAMMS, and a regeneration in the presence of reducing agents may restore the thiol group to its reduced state and recover the full capacity of the SAMMS.

5. Second Regeneration: 0.095 g of mercury-SAMMS (dried overnight) was added to 10.0 mL high purity concentrated HCl solution for 4 hours. The solid SAMMS was then separated by filtration. By analyzing the mercury concentration in the filtrate and comparison with the available mercury on the SAMMS, the bound mercury was found 100% released from the SAMMS.

6. Third loading with mercury: The regenerated SAMMS was washed with high purity water thoroughly and air-dried overnight. A 0.069-g quantity of regenerated SAMMS was added to 137 mL of 0.1 M $NaNO_3$ solution containing 330 mg Hg/L, and the mixture was agitated for 4 hours at room temperature. The mixture was filtered, and the mercury-SAMMS powders were washed with high purity water and air-dried overnight. By analyzing the mercury concentrations of the blank solution and the final solution, a mercury loading of 233 mg Hg/g of SAMMS was obtained, which was again about 50% of the original capacity. This may suggest no further oxidation of the SAMMS. The regeneration experiments will be repeated in the future with the presence of reducing agents.

The mercury-laden SAMMS, therefore, can be regenerated with concentrated HCl. The first treatment resulted in almost 100% release of the bound mercury. The regenerated mercury recovered only 50% capacity. The second regeneration showed again 100% release of mercury. The SAMMS after the second generation showed again a 50% of the original capacity in its third time in binding mercury. The complete regeneration of the SAMMS may need reducing agents. A 2 N HCl solution can release only 14% of the bound mercury.

5.0 Preliminary Cost Estimate

5.1. Background

The Nonradiological Wastewater Treatment Plant (NRWTP) at the Oak Ridge National Laboratory currently treats wastewater to remove hazardous metals and organics before discharge to nearby creeks. Changes in the NPDES permit may require treatment to very low levels of mercury (12 ppt). The current treatment system uses activated carbon to remove low levels of organics and mercury, but the effluent generally does not meet the 12-ppt limit. New highly selective separations materials offer an attractive way to meet the lower discharge limits.

5.2 Purpose and Scope

The purpose of this section is to develop and document preliminary costs for applying the SAMMS materials to remove mercury. The focus of this effort is on removing mercury from wastewater treated at the NRWTP. Additional applications of SAMMS for mercury removal, such as those at the Y-12 plant, will be addressed in follow-on studies.

5.3 Approach

To develop cost estimates for implementing SAMMS for mercury removal requires that implementation methods be developed and assessed. The alternatives considered include 1) install a separate column system using SAMMS, 2) mix the SAMMS with the activated carbon in the existing columns, or 3) use a small skid mounted system with SAMMS for treatment at the source. Given the laboratory-scale status of the development of the SAMMS materials, an accurate cost estimate for production and implementation of SAMMS is difficult to provide. The uncertainties are minimized by developing cost estimates that are incremental to the existing treatment operation. A rough cost estimate for the production of commercial quantities of the materials was developed by determining the bulk cost of the chemicals required for synthesis and by obtaining costs of other separations materials that have some synthesis steps in common with the SAMMS.

5.4 Mercury Removal at the Nonradiological Wastewater Treatment Plant

This section contains the available cost information on SAMMS and applying SAMMS to the removal of mercury at the NRWTP. A description of the existing system is included along with a discussion of three alternatives for using SAMMS to meet the new effluent limit of 12 ppt for mercury.

5.4.1 Description of the Existing Mercury Removal System

The NRWTP treats water at an average rate of 1200 Lpm (320 gpm), which corresponds to a total annual volume of 637 million L (168 million gallons). There are numerous sources of the contaminated water, including building sumps and runoff and ground water. The flow to the NRWTP is variable due to rainfall, so the plant is sized for a maximum capacity of 2880 Lpm (760 gpm). The most concentrated

mercury sources are the building sumps where historical spills occurred. The flow to these sumps is from in leakage of groundwater and rainwater is highly variable and is roughly estimated to be in the range of 4 to 76 Lpm (1 to 20 gpm). The mercury concentration varies from less than 0.0002 mg/L to a maximum of 0.8 mg/L for individual sump samples. Concentrations of mercury in the wastewater feed to the NRWTP are not available at this time.

The existing system in use at the NRWTP for treating the wastewater involves a number of sequential process steps that include chemical precipitation, clarification, filtration, air stripping, and activated carbon adsorption. Much of the heavy metal content, including some mercury, is removed in the precipitation step and separated from the bulk liquid in the clarification and filtration steps. Other important heavy metals that are partially removed include arsenic, chromium, copper, lead, nickel, selenium, silver, and zinc. Volatile organics are removed by the air stripping step. Activated carbon, which removes low levels of organics and mercury, is used to polish the water before it is discharged.

A typical operation uses three columns of activated carbon: two columns operate in series with a third on standby. Each column contains 9900 kg (22,000 lb) (239 m^3 [785 ft^3]) of activated carbon. The mercury concentration in the feed to the activated carbon beds typically ranges from 200 ppt to 400 ppt with an average close to 200 ppt. The mercury level in the effluent from the activated carbon beds is typically less than 50 ppt, but is sometimes detected at concentrations up to 100 ppt. Consequently, the plant as currently configured and operated does not meet the new effluent requirement for mercury (12 ppt). The spent carbon is disposed of as low level waste at a cost of $60/ft^3$. The carbon is handled as LLW because it is slightly contaminated with ^{137}Cs, ^{90}Sr, and ^{60}Co. It is assumed that a carbon bed will process 2 years worth of wastewater and that the activated carbon amount is determined by the organic removal requirement. The annual carbon requirement is 11,000 lb, and the annual cost is $9400 (@$0.85/lb). The total disposal cost of the carbon on an annual basis is $23,500/yr.

5.4.2 Description of Mercury Removal Using SAMMS

To develop cost information, it is necessary to develop implementation alternatives. The following three alternatives for implementing the SAMMS for mercury removal at the NRWTP are considered: 1) install a separate column system using SAMMS, 2) mix the SAMMS with the activated carbon in the existing columns, 3) use a small skid-mounted system with SAMMS for source treatment.

5.4.2.1 Separate Column System Using SAMMS

In this alternative, it is proposed that a separate three-column system would be installed to treat the full amount of wastewater:1213 Lpm (320 gpm). Two of the columns would be placed in series with one column on standby. Two columns in series allows nearly complete loading of the first column while maintaining high decontamination factors for the mercury. The third column on standby would allow changeout of the mercury-loaded SAMMS without interrupting water treatment. Calculations based on isotherm data suggest that 1.6 kg of SAMMS should be sufficient for 1 year of operation. If it is assumed that the SAMMS can be fully loaded (i.e., in equilibrium with the feed at 0.0002 ppm), the mercury loading on the SAMMS is about 80 mg Hg/g of SAMMS. One year of wastewater contains about 127,000 mg of mercury. Dividing this value by the loading assumed for the SAMMS gives 1590 g or about 1.6 kg.

The difficulty with this approach is attempting to contact such a large volume of water with a small volume of SAMMS in a column operation. Attempting to force such a large volume of water through a

small bed volume would result in excessive pressure drop and would probably provide an inadequate residence time for the mercury removal process (i.e., 0.08 s at 1213 Lpm [320 gpm]). For comparison, the activated carbon beds are sized to provide a residence time of 7.75 min (7.75 bed volumes/h). Preliminary data indicate that the SAMMS have rapid kinetics for removing mercury, so the required column size may be less than the size of the carbon beds. In the absence of column testing data, it is not possible to accurately project a size for the columns.

Assuming the SAMMS are implemented in a 3-column system similar to the existing system (2 columns in series and 1 on standby), the capital cost is estimated to be about $5M. This estimate was developed using cost data developed in the PAI Corporation engineering study. The columns are greatly over sized for this application, but this is necessary to avoid excessive pressure drops. While the column size can undoubtedly be made smaller, the costs would still be substantial. Assuming the columns are reduced in size by a factor of 10 and assuming the capital cost varies with an exponent of 0.6, the capital cost would still be $1.25M. Operating and maintenance costs for an extra ion exchange system were estimated to be about $100k/yr

5.4.2.2 Mix with the Activated Carbon

In this alternative, it is proposed that the SAMMS would be mixed with the activated carbon and used in the existing equipment. The activated carbon would remove the trace amounts of organics, and the SAMMS would enhance the mercury removal capability. In the absence of experimental data, it is difficult to accurately project the amount of SAMMS that would be required to adequately enhance the mercury removal capability, but 1 to 10 wt% seems reasonable. At the West Valley Demonstration Project (West Valley, New York), about 10 wt% titania is added to zeolite, to remove trace amounts of transuranics in addition to the cesium. However, the titania-loaded zeolite was only needed in every third or fourth column. With 9900 kg (22,000 lb) of activated carbon per column, the SAMMS requirement is 99 to 990 kg (220 to 2200 lbs) per column.

The capital cost of this approach would be $0 since existing equipment would be used. Operating and maintenance costs would remain unchanged since neither operations nor equipment would be changed. The only additional costs would be for the SAMMS materials and a small incremental amount for waste disposal associated with the additional volume due to the SAMMS. Assuming the activated carbon requirement remains unchanged, a SAMMS loading of 1 to 10% of the activated carbon, and a cost of $50/kg for the SAMMS, the purchase cost of the SAMMS would range from $2500/yr to $25,000/yr. The incremental cost of waste disposal would range from 1 to 10% of the current cost for disposal or $235 to 2,350/yr. Adding this to the cost of the SAMMS and rounding off to one significant figure gives a total incremental cost of $3k/yr to $30k/yr.

5.4.2.3 Small System for Source Treatment

In this alternative, it is proposed that the SAMMS would be implemented in a small skid-mounted unit for removal of mercury at the source. This would allow a much smaller volume of water to be more easily contacted with the small volumes of SAMMS. The mercury loading on the SAMMS could also be improved because the mercury concentration is greater in the source streams. Two types of units are considered; skid-mounted columns and 3M cartridges.

The skid mounted unit with columns is assumed to have 3 columns in series (2 in series and 1 on standby). Two columns would be online with one on standby. Each column would contain about 13 ft^3

(368 L) of SAMMS and are sized to operate with a flowrate of 12.5 bed volumes per hour. The skid would also include a sand filter, surge tank, pumps, and automated valve switching. This skid is estimated to cost $65k based on a vendor quote. A separate quote of $18k was obtained for a manually operated system with similar components. It is assumed that the SAMMS would be used on a once-through basis and disposed of as LLW.

The total amount of SAMMS for a 3-column system is 39 ft^3 (1100 L) and would cost about $55k, bringing the total capital cost to $120k (skid + SAMMS). Based on equilibrium considerations, this probably is a large amount of SAMMS for the amount of mercury present. Based on the feed to the activated carbon columns (which contains an estimated 127 g of Hg/yr and requires an estimated 1.6 kg of SAMMS), each of the skid-mounted columns could theoretically treat 230 years of wastewater. The actual SAMMS requirement for source treatment may be somewhat greater than 1.6 L/yr, but an accurate estimate requires the results of an ongoing effort to characterize the source flowrates and mercury concentrations. The cost to dispose of a 13 ft^3 column is estimated to be about $780, which is a negligible annual cost. Since these units would be separate from the NRWTP, additional labor costs would be incurred. These are estimated at 0.5 to 1 FTE for an incremental operational cost of $100k-$200k.

The 3 M cartridges have been specifically designed to allow highly selective sorbents and ion exchange materials to be contacted with large amounts of water containing dilute levels of contaminates. The cartridges contain web material that supports small particles of the separations media. The support structure allows rapid flow without excessive pressure drop, and the small particles allow rapid diffusion in the particle. Skid mounted cartridges have been used to remove ^{90}Sr from N-Springs groundwater at the Hanford site (Brown et al. 1996), to remove radioactivity from evaporator overheads at the West Valley Demonstration Project (Dinsmore et al. 1996) and to remove radioactivity from groundwater at the Idaho Site (Brewer, 1995). The units that have been used have a capacity of 37.9 Lpm (10 gpm) and contain a sorbent mass of 857 g and cost $52k. Two units would be required for 75.8 Lpm (20 gpm) for a total capital cost of $104k. Assuming the cartridges would need to be changed out twice per year (1.6 kg of SAMMS), the cost of the SAMMS would be $80/yr. Each cartridge has a volume of about 1.7 L. With 12 cartridges requiring disposal every year, the volume is 1 ft^3, and the disposal cost would be $60/yr. Since these units would be separate from the NRWTP, additional labor costs would be incurred. These are estimated at 0.5 to 1 FTE for an incremental operational cost of $100k-$200k.

5.5 Comparison of Costs

The cost estimates developed in this study are compared to cost estimates obtained from the PAI Corp study (Table 5.1). These costs are incremental, relative to existing operations. While considerable uncertainty is associated with these estimates, it is apparent that the use of SAMMS has the potential to provide improved mercury removal for the least cost. The options considered in the PAI corp study involve substantial upgrades and additions to the NRWTP or completely new capabilities and therefore involve considerable capital and operating expense.

5.6 Material-Lifetime Cost Comparison

Given the uncertainty associated with the cost estimates for implementation, it is instructive to compare the costs associated with the use of the separations materials and waste disposal. This is shown in Table 5.2, where the costs are developed for removing 1 kg of mercury. The amount of SAMMS material

is based on laboratory equilibrium data at a mercury concentration of 200 ppt. The amount of GT-73 material is based on an extrapolation of manufacturers data to 200 ppt from higher concentrations. The amount of activated carbon is based on the performance of the full-scale columns. In the absence of capital and labor costs, it is apparent that the SAMMS are the most economical sorbent material for mercury removal.

Table 5.1. Comparison of Costs

	Capital, $M	Operating and Maintenance, $M/yr
Dilute to river	18.5	0.37
Flow augmentation	7.7	0.37
Alternative A	1.15	0.57
Alternative B	3.09	0.66
Alternative C	3.91	0.82
Alternative B + IX/Evap	7.32	1.15
Alternative C + IX/Evap	8.15	1.31
Alternatives for implementing SAMMS		
Separate column system	1.25-5.0	0.1-0.2
Mix SAMMS with Activated Carbon	0	0.003-0.03
Skid mounted columns	0.12	0.1-0.2
Skid mounted 3 M cartridges	0.104	0.1-0.2

5.7 Cost Summary

The preliminary cost information developed in this report indicates that SAMMS offers a method for improved mercury removal that may be significantly less expensive than other options. The SAMMS is less expensive because of the relatively high mercury loading that can be achieved. This reduces the capital cost by reducing the size of the treatment system and by reducing the waste disposal volume. Also, contributing to a reduced cost is the fact that the SAMMS can be implemented as a one-time-use sorbent and then disposed of directly as a waste form. This mode of operation is relatively simple, resulting in reduced operating costs, and avoids the costs associated with secondary waste treatment.

Table 5.2. Material-Lifetime Cost Comparison

	SAMMS	GT-73	Activated Carbon
Material Cost, $/kg	$50/kg	$42/kg	$1.78/kg
Hg loading, g/kg @ 0.2 ppb	80 g/kg	6.5 g/kg	0.025 g/kg
Material Required for Removal of 1 kg of Hg	13 kg	154 kg	40,000 kg
Waste Disposal Cost per Kg of Hg Removed @ $60/ft^3	$60	$489	$190,000
Total cost per kg of Hg removed	$710	$6960	$261,000

The preliminary cost estimates for implementing SAMMS for mercury removal at the NRWTP are summarized in Table 5.3. These estimates are significantly less than the estimates associated with other options that have been evaluated. Estimates for upgrading or adding to the NRWTP include capital costs that range from $1.1.5M to $8.15M and annual operating costs that range from $0.57M to $1.31M (PAI Corp.). The most expensive system evaluated had a capital cost of $18.5M and involved developing infrastructure to allow the wastewater to be diluted in a high flow river.

A rough cost estimate for the production of commercial quantities of the materials was developed by determining the bulk cost of the chemicals required for synthesis and by obtaining costs of other separations materials that have some synthesis steps in common with the SAMMS. The cost of the raw materials obtained in bulk were determined to be $20.77/kg of SAMMS with a market price estimated to be approximately $50/kg or $1400/ft^3. This cost estimate may be compared to other separations materials that range from $29/kg for zeolite beta to $100/kg for crystalline-silico titanates (a cesium ion exchange material) to thousands of dollars per kg for high grade chromatography materials produced in relatively low quantities.

A comparison of the cost of the materials and waste disposal reflects the high capacity and selectivity of the SAMMS. The cost per kg of mercury removed was estimated to be $710 for the SAMMS, $6960 for GT-73 (a commercially available organic based sorbent), and $261,000 for activated carbon. The high mercury loading on the SAMMS results in a small volume of material, minimizing the cost of material procurement and waste disposal.

A key issue in realizing the economy offered by SAMMS is to implement the materials in a manner that efficiently contacts the SAMMS with the wastewater and takes advantage of the highly selective characteristics of the SAMMS. The most promising options for achieving this are to mix the SAMMS with the existing activated carbon beds or to implement the SAMMS in small skid-mounted units for source treatment that involves smaller volumes of wastewater. Implementing the SAMMS in a large traditional column system appears to be as costly as other methods that have been considered and would be hugely oversized for the application.

Table 5.3. Preliminary Cost Estimates for Implementing SAMMS for Mercury Removal

	Capital Cost, $M	**Operating and Maintenance, $M/yr**
Separate column system	1.25-5.0	0.1-0.2
Mix SAMMS with activated carbon	0	0.003-0.03
Skid mounted columns	0.12	0.1-0.2
Skid mounted 3 M cartridges	0.104	0.1-0.2
NonSAMMS Alternatives	1.15-18.5	0.57-1.31

6.0 Conclusions

The data discussed above may provide some indications that SAMMS technology has the following characteristics.

1. *High RCRA Metal Loading*: The high surface area of the mesoporous oxides (>1000 m^2/g) ensures large capacity for metal loading (up to 0.64 g Hg/g of SAMMS).

2. *High Selectivity*: Self-assembled functional groups provide the high selectivity for RCRA metals, such as Hg, Ag, Pb, and Cd, without significant interference from other abundant cations (such as alkali and alkaline earths) and anions such as Cl^-, CO_3^{2-}, SO_4^{2-}, and PO_4^{3-} in wastewaters. There are almost no pH effects on the mercury binding of SAMMS between pH 4 and 9. At pH 2 and 10, the Kd of SAMMS for mercury may be reduced by more than 10 times, and the pH 2 had a larger effect than that at pH 10. Almost no ionic strength effects have been observed on the Kd of SAMMS for mercury between 0 and 4 M $NaNO_3$ solutions.

3. *High Affinity*: The covalent binding between the thiol group of SAMMS and mercury provide the high affinity for mercury so that SAMMS is capable of reducing the mercury concentrations in salt solution and in groundwater below a 10-ppt level (the detection limit of the mercury analyzer).

4. *Fast Kinetics*: The high surface area on SAMMS and high affinity of its functional group for mercury result in fast binding kinetics so that SAMMS can reduce a 0.5 ppm mercury in 0.1 M $NaNO_3$ solution to 0.5 ppb in less than 5 minutes at a solution-to-SAMMS ratio of 2000. The kinetics in engineered SAMMS, such as beads and membranes, are to be investigated next year.

5. *High Flexibility*: SAMMS binds mercury in different forms, including metallic, organic, ionic, neutral such as $Hg(OH)_2$ (aq), and complexes such $HgCl_2$; removes mercury from aqueous wastes, organic oils, and mercury vapor; is expected to be applicable also to sludges and soils (which is going to be demonstrated in a project funded by DOE MWFA); and is demonstrated to be effective in pH 2 to 10. SAMMS removed 91% of the Hg in SRS tritiated pump oils waste through a single treatment with SAMMS powders.

6. *Permanent Waste Form*: The mercury-loaded SAMMS not only can pass TCLP tests, but also has good chemical durability as a permanent waste form because 1) the covalent binding between mercury and SAMMS has good resistance in ion exchange, oxidation (up to 150°C in air), and hydrolysis (up to 70°C in water) and 2) the uniform and small pore size (2 to 40 nm) of the mesoporous silica prevents bacteria (at least 2000 nm in size) from solubilizing the bound mercury (microbes are mainly responsible for solubilizing the mercury compounds in the environment into the deadly methylmercury). The SAMMS technology is superior to many existing technologies because of the direct generation of a stable waste form that does not require secondary treatment.

7. *No Secondary Wastes*: During the application of SAMMS and disposal of merucry-SAMMS, no secondary wastes are generated, the mercury-SAMMS can be disposed of as nonhazardous waste, and the final waste volume is small because of the high waste loading of SAMMS.

8. *Regenerability*: SAMMS can be regenerated using concentrated HCl if such needs exist. This may be useful for some special applications such as using SAMMS as a mercury sensor.

9. *Multiple Applicability*: SAMMS with different functional groups is being shown to be effective in removing cations such as Pb, Cd, and Ag, actinides Pu, Np, and Am (Feng et al. 1998), anions such as As, Cr, and Re, and organics such as dense nonaqueous phase liquids (DNAPLs) (Liu et al. 1997).

10. *Low Cost Implementation*: The preliminary cost assessment of the SAMMS technology for RCRA metal removal indicates a lower lifetime cost than existing technologies.

7.0 References

Anthony RG, CV Philips, and RG Dosch. 1993. *Waste Management* **13**, 503.

Attard GS, JC Glyde, and CG Gottner. 1995. *Nature*, **378**, 366.

Badia A, et al. 1996. *Langmuir* **12**, 1262.

Baes, CF. Jr., and RE. Mesmer, 1976, *The Hydrolysis of Cations*, John Wiley & Sons, New York

Bagshaw SA, E Prouzet, and TJ Pinnavaia. 1995. *Science*, **269**, 1242.

Ball P. 1994. *Designing the molecular world*, Princeton University Press: Princeton, New Jersey.

Beck JS, JC Vartuli, WJ Roth, ME Leonowicz, CT Kresge, KD Schmitt, C T-W Chu, DH Olson, EW Sheppard, SB McCullen, JB Higgins, and JL Schlenker. 1992. *J. Am. Chem. Soc.* **114:**10834.

Beck JS., and JC Vartuli. 1996. *Cur. Opin. Sol. St. Mater. Sci.* **1,** 76.

Blayney, M.B., J. S. Winn, D. W. Nierenberg, *1997, Chem & Eng News*, 12 May, 7

Brown GN, KJ Carson, JR DesChane, RJ Elovich, TM Kafka, and LR White. 1996. *Ion exchange removal of strontium from simulated and actual N-Springs well water at the Hanford 100-N Area.* PNNL-11198, Pacific Northwest National Laboratory, Richland, Washington.

Brewer KN, TA Todd (Lockheed Idaho Technologies Company), TM Kafka and LR White (3M), and LA Bray (PNL). 1995. *Decontamination of TAN Injection Well Water Using 3M Web Technology,* INEL-95\0589, Lockheed Idaho Technologies Company, Idaho Falls, Idaho.

Bunker, BC, PC Rieke, BJ Tarasevich, AA Campbell, GE Fryxell, GL Graff, L Song, J Liu, and JW Virden. 1993. "Ceramic Thin Film Formation on Functionalist Interfaces Through Biomimetic Processing," *Science*, **261**, 1286.

Dinsmore EF, G Smith, LABray, GN Brown, KC Carlson, TM Kafka, DCSeely, and LR White. 1996. *Removal of specific radionuclides from process streams at the West Valley demonstration project using 3M separation technology.* 3M New Products Department, St. Paul, Minnesota.

Feng X, J Liu, and GE Fryxell. 1997a. "Self-assembled Mercaptans on Mesoporous Silica (SAMMS) for Mercury Separation and Stabilization," U.S. Patent Application filed on February 7, 1997a, PNNL #E-1479.

Feng X, GE Fryxell, LQ Wang, AY Kim, J Liu, and KM Kemner. 1997b. "Functionalized Monolayers on Ordered Mesoporous Supports," *Science, 276*, 923-926.

Feng X, L Rao, TR Mohs, GE Fryxell, Y Xia, J Lu, J Xu, and KN Raymond. 1998. "Removal of Am(III), Th(IV), Np(V), and U(VI)from Wastewater Using SAMMS," accepted for presentation at AIChE's 1998 Spring National Meeting, March 8-12, New Orleans, Louisiana.

Firouzi A, et al. 1995. *Science*, **267**, 1138.

Fryxell GE, PC Rieke, LL Wood, MH Engelhard, RE Williford, GL Graff, AA Champbell, RJ Wiacek, L Lee, and A Halverson. 1996. "Nucleophilic displacements in mixed self-assembled monolayers." *Langmuir* **11**, 318-326.

Gao W, and L Reven. 1995. *Langmuir* **11**, 1860-1863.

Ghazy SE. 1995. "Removal of Cadmium, Lead, Mercury, Tin, Antimony, and Arsenic from Drinking and Seawaters by Colloid Precipitate Flotation," *Sep. Sci. Technol.*, **30**(6):933.

Huo Q, et al. 1994. *Nature*, **368**, 317.

Kresge CT, ME Leonowicz, WJ Roth, JC Vartuli, and JS Beck.. 1992. *Nature* **359:**710.

Kumar A, HA Biebuyck, and GM Whitesides. 1994. *Langmuir,* **10**, 1498.

Larson KA and JM Wiencek.. 1994. "Mercury Removal from Aqueous Streams Utilizing Microemulsion Liquid Membranes," *Environmental Progress,* 13(4):253.

Le Grange JD, JL Markham, and CR Kurkjian. 1993. *Langmuir*, **9**, 1749-1753.

Levy GC, RL Lichter, and GL Nelson. 1980. *Carbon-13 Nuclear Magnetic Resonance Spectroscopy*, 2nd Ed., John Wiley and Sons, New York.

Liu J., et al. 1996. *Adv. Colloid. Interface. Sci.* **69**, 131.

Liu J, G Fryxell, X Feng, and R Hallen. 1997. PNNL 1997 APTI Laboratory Initiative Project.

Maschmeyer T, F Rey, G Sankar, and JM Thomas. 1995. *Nature*, **378**, 159.

Mitra S. 1986. Mercury in the ecosystem, Trans Tech Publications, USA

Otanl Y, H Eml, C Kanaoka, and H Nishino. 1988. "Removal of Mercury Vapor from Air with Sulfur-Impregnated Adsorbents," *Environ. Sci. Technol.*, 22(6):708.

Pai Corporation. 1993. *Non-radiological Wastewater Treatment Plant Upgrade Options for Compliance with Water Quality-Based Effluent Standards*, PAI Corporation and AquAeTer, Inc.

Ritter JA and JP Bibler. 1992. Toxic Waste Management in the Chemical and Petrochemical Industries., "Removal of Mercury From Waste Water: Large-scale Performance of An Ion Exchange Process," *Water Sci. Technol.*, **25**(3):165.

Sayari A. 1996. *Chem. Mater.* **8**, 1840.

Sayers DE and BA Bunker. 1988. *X-Ray Absorption, Principles, Applications, Techniques of EXAFS, SEXAFS, AND XANES.* D. C. Koningsberger and R. Prins, Eds. [Wiley and Sons Publishing Co. New York], pp. 211-256 and all of chapter 6.

Schierbaum KD. 1994. *Science* **265**, 1413.

Schwarzenbach G and M Schellenberg. 1965. *Helv. Chim. Acta*, **48**, 28.

Stern EA and SM Heald. 1979. *Rev. Sci. Instrum* **50**, 1579.

Sindorf, D. W. and G. E. Maciel, *J. Am Chem. Soc.* **105**, 3769 (1983).

Tanev PT and TJ Pinnavaia. 1995. *Science*, **267**, 865.

Tarasevich BJ, PC Rieke, and J Liu. 1996. "Nucleation and Growth of Oriented Films onto Organic Interfaces," *Chemistry of Materials*, **8**: 292-300.

Tripp CP and ML Hair. 1992. *Langmuir* **8**, 1120-1126.

Sindorf DW and GE Maciel. 1983. *J. Am Chem. Soc.* **105**, 3769.

Tian Z, W Tong, J Wang, N Duan, VV Krishana, and SL Suib. 1997. *Science*, **276**, 926.

Ulman A, SD Evans, Y Shnidman, R Sharma, JE Eilers, and JC Chang. 1991. *J. Am. Chem. Soc.*, **113**, 1499.

Wang L-Q, J Liu, GJ Exarhos, and BC Bunker. 1996. *Langmiur* **12**, 2663.

Wirth MJ, RW Peter Fairbank, and HO Fatunmbi. 1997. *Science*, **275**.

8.0 Patents Publications and Press Highlights

Patents:

Feng X, J Liu, and GE Fryxell. 1997. "Self-assembled Mercaptans on Mesoporous Silica (SAMMS) for Mercury Separation and Stabilization," U.S. Patent Application filed on February 7, 1997, PNNL #E-1479.

Publications:

Feng X, GE Fryxell, LQ Wang, AY Kim, J Liu, and KM Kemner. 1997. "Functionalized Monolayers on Ordered Mesoporous Supports," *Science*, *276*, 923-926.

Feng X, JLiu, and GE Fryxell. 1997. "Self-Assembled Monolayers on Mesoporous Supports (SAMMS) for RCRA Metal Removal," Proceedings of Efficient Separations and Processing Crosscutting Program 1997 Technical Exchange Meeting, January 28-30, 1997, Gaithersburg, Maryland, PNNL-SA-28461, 5.15-5.20.

Press Highlights:

Science highlighted SAMMS technology for mercury removal in "*This Week In Science*" on 9 May 1997.

Chemical & Engineering News published a feature article on 19 May 1997 to hail the SAMMS material as a "supersoaker for heavy metals."

Scientific American (October 1997) featured SAMMS in the "*Technology and Business" section* as a breakthrough material that "can render hazardous wastewater clean enough to drink."

Appendix A
Production Cost Estimate for SAMMS

Appendix A
Production Cost Estimate for SAMMS

The production cost of SAMMS was estimated by obtaining estimates from chemical suppliers of the raw materials in bulk. The details of this estimate may be found in Table A1 where the total cost of raw materials is estimated to be $20.77/kg of SAMMS. Considering a number of other cost factors, a value of $50/kg for the production of SAMMS in bulk is considered reasonable. This corresponds to a volumetric cost of $1400/ft^3, assuming a dry density of 1 kg/L for the engineered form of SAMMS.

As a check on the reasonableness of this estimate, several producers of separations materials were queried as to their costs. One vendor, who wishes to remain anonymous, indicated that their production costs of separations materials are typically; $40,000/ft^3 for gram quantities, $20,000/ft^3 for kg quantities, $2000 to $3000/ft^3 for a few cubic feet and upper 100s to lower 1000s for 1000 ft^3. Another vendor in the business of producing functionalized silica beads for chromatography applications indicated costs that ranged from $400/kg to $4000/kg. These materials are more expensive than the estimate for SAMMS, but are not produced in large quantities and often require high grade and expensive silica. A final example is Zeolite beta, which is made using an organic template similar to the production of SAMMS. The price was quoted as $29/kg, which is quite high for zeolites. It can be seen that the cost estimate of $50/kg ($1400/ft^3 of SAMMS is consistent with the costs of these separations materials.

Table A-1. Raw Material Cost for SAMMS

Chemical	Source of quote	Basis amount, lb	Price $/lb	Shipping, $/lb	Delivered Price **, $/lb	Delivered price, $/kg	Amount, kg	Cost per kg of SAMMS $/kg
29wt% CTAC	LONZA Inc.	40,000	0.74	0.06	0.80	1.76	2.436	4.29
Sodium Aluminate (dry)	Pfaltz and Bauer	40,000	8.60	0.06	1.29	2.84	0.0528	0.15
HiSil 233	PPG	30,000	0.65	0.07	0.72	1.57	0.3036	0.48
Soluble silicate, 38wt% SiO_2:Na_2O	PQ	20,000-40,000	0.08	included	0.08	0.18	0.448	0.08
3-mercaptopropyltrimethoxysilane	HULS America	40,000	10.00	Included	10.00	22.03	0.716	15.77
							Total	$20.77/kg
								$588.22/ft^3

** Shipping is based on $1.10/mile and 2000 miles (by truck)

Distribution

No. of Copies

Offsite

2 DOE/Office of Scientific and Technical Information

John Mathur
U.S. Department of Energy
Office of Science and Technology
Germantown, MD 29874

Jerry L. Harness
U.S. Department of Energy
3 Main Street
Oak Ridge, Tennessee 37830-8620

G.C.S. Ordaz
U.S. Department of Energy
Office of Science and Technology
Germantown, MD 29874

Helen Farrell
ER-13
U.S. Department of Energy
Germantown, MD 20874-1290

Jack S. Watson
Oak Ridge National Laboratory
P.O. Box 2008
Oak Ridge, TN 37831

K. T. Klasson
Oak Ridge National Laboratory
P.O. Box 2008
Oak Ridge, TN 37831

Tom Conley
Oak Ridge National Laboratory
P.O. Box 2008
Oak Ridge, TN 37831

Greg Hulet
Lockheed Martin Idaho Technologies Co.
PO Box 1625
Idaho Falls, ID 83415-3875

Dirk Gombert
Lockheed Martin Idaho Technologies Co.
PO Box 1625
Idaho Falls, ID 83415

Jay Roach
Lockheed Martin Idaho Technologies Co.
PO Box 1625
Idaho Falls, ID 83415

M. J. Steindler
Argonne National Laboratory
Bldg. 205
9700 S. Cass Avenue
Argonne, IL 60439-4837

J. K. Bates
Argonne National Laboratory
Bldg. 205
9700 S. Cass Avenue
Argonne, IL 60439-4837

J. C. Cunnane
Argonne National Laboratory
Bldg.205
9700 S. Cass Avenue
Argonne, IL 60439-4837

M. C. Thompson
Westinghouse Savannah River Co.
Savannah River Technology Center
P.O. Box 616
Aiken, SC 29802

C. M. Jantzen
Westinghouse Savannah River Co.
Savannah River Technology Center
Bldg 707-C, P.O. Box 616
Aiken, SC 29808

I. L. Pegg
The Catholic University of America
Vitreous State Laboratory
620 Michigan Avenue, N.E.
Washington, DC 20064

D. F. Bickford
Westinghouse Savannah River Co.
Savannah River Technology Center
Bldg 707-C, P.O. Box 616
Aiken, SC 29808

A. Barkatt
The Catholic University of America
Vitreous State Laboratory
620 Michigan Avenue, N.E.
Washington, DC 20064

Y. N. Chiu
The Catholic University of America
Vitreous State Laboratory
620 Michigan Avenue, N.E.
Washington, DC 20064

J. B. Hunt
National Science Fundation
4201 Wilson Blvd.
Arlington VA 22230

R. E. Sassoon
Science Applications International Co.
555 Quince Orchard Rd. Suite 500
Gaithersburg, MD 20878

R. E. Sassoon
Science Applications International Co.
555 Quince Orchard Rd. Suite 500
Gaithersburg, MD 20878

P. Hart
U.S. Department of Energy
MS-E06
P.O. Box 880
Morgantown, WV 26507-0880

B. M. Frankhouser
U.S. Department of Energy
3610 Collins Ferry Rd
PO Box 880
Morgantown, WV 26507-0880

Norman Li
50 E. Algonquin Rd.
Des Plaines, IL 60017

Rod Ewing
Dept Nuclear Engineering and
Radiological Sciences
The University of Michigan
2355 Bonisteel Boulevard
Ann Arbor, Michigan 48109-2104

W. Lutze
University of New Mexico
Department of Chemical and Nuclear
Engineering, Farris Engineering Center
Room 209
Albuquerque, NM 87131-1341

D. M. Strachan
Argonne National Laboratory
Chemical Technology Division
9700 S. Cass Avenue
Argonne, IL 60439-4837

D. Clark
University of Flordia
Dept of MSE
136 MAE, PO Box 116400
Gainesville, FL 32611-6400

No. of Copies

T. M. Kafka
3M Center, Bldg. 209-1W-24
St. Paul, MN 55144-1000

S. L. Stein
Greenhill Technologies
PO BOX 5395
4000 NE 41st St.
Seattle, WA 98105-5428

P. J. Usinowicz
505 King Avenue
Columbus, Ohio 43201-2693

W.C. MacDonald
505 King Avenue
Columbus, Ohio 43201-2693

S. Cohen
505 King Avenue
Columbus, Ohio 43201-2693

W.W. Simmons
505 King Avenue
Columbus, Ohio 43201-2693

N. K. Chung
Metcalf & Eddy
30 Harvard Mill Square
PO Box 4071
Wakefield, MA 01880-5371

Ken M. Kemner
Argonne National Laboratory
9700 S. Cass Ave.
Argonne, IL 60439

No. of Copies

Onsite

4 **DOE Richland Operations Office**

T. L. Aldridge, K8-50
R.A. Pressentin, K8-50
S.N Saget, K8-50
D. A. Brown, K8-50

62 **Pacific Northwest National Laboratory**

E. G. Baker, K2-12
S. Baskaran, K2-44
Bill Bonner, K9-14
Jim Buelt, P7-41
B. C. Bunker, K2-45
X. Feng, P8-37 (30)
G. E. Fryxell, K2-44
C. S. Ghormley, P8-37
M. Gong, P7-41
R. T. Hallen, K2-12
Bill Kuhn, K8-93
D. E. Kurath, P7-28
Jun Liu, K2-44
Mike Lilga, P8-38
Nick Lombardo (6)
S. V. Mattigod, K6-81
Z. Nie, K2-44
Joe Perez, P7-41
John Sealock, K2-10
Terri Stewart, K9-69
Rod Quinn, K9-69
Jud Virden, K2-44
L-Q. Wang, K2-44
Technical Report Files (5)